

HTRA II :

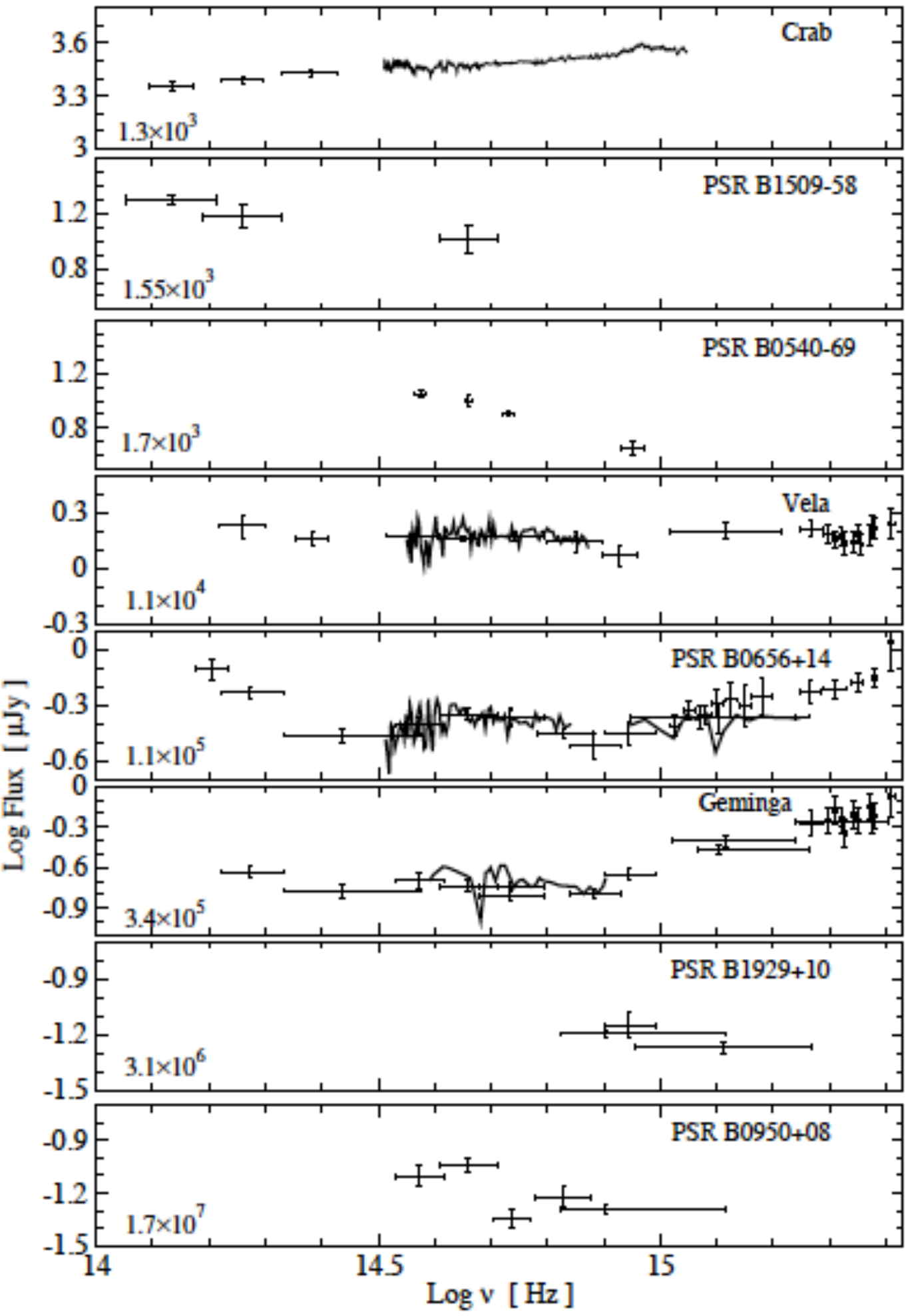
Andy Shearer
Centre for Astronomy
NUI, Galway
on behalf of the Opticon HTRA network



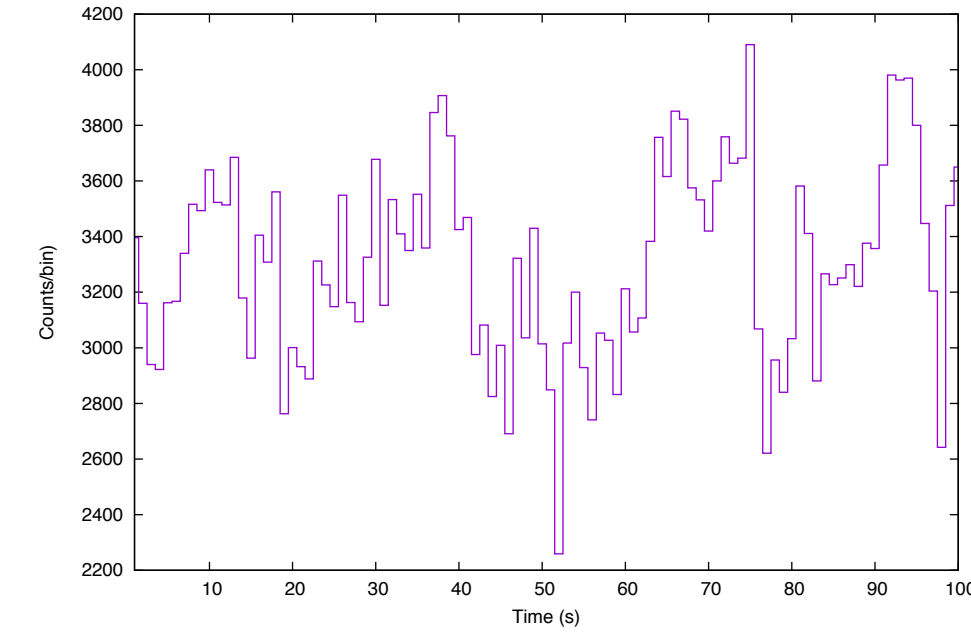
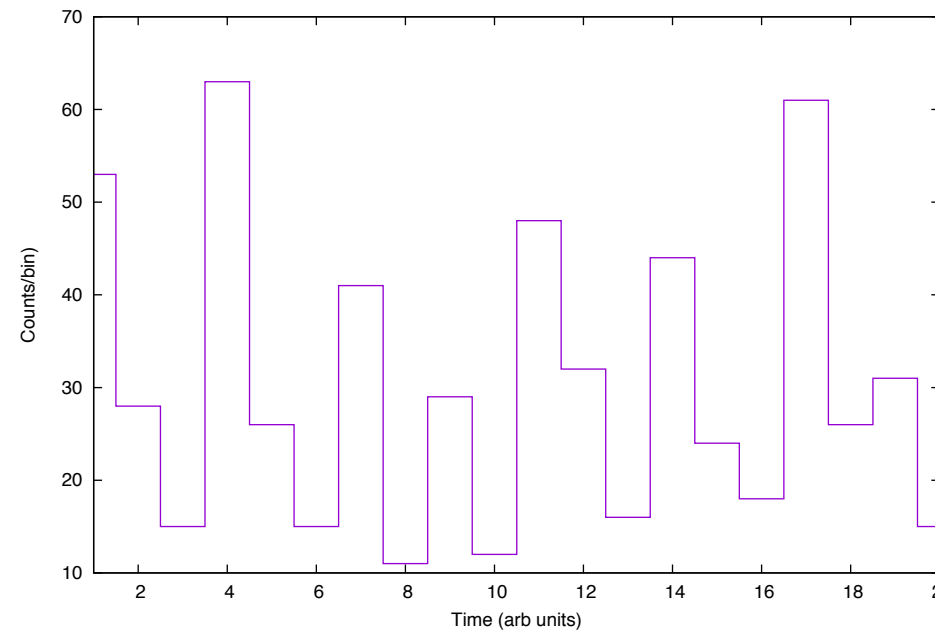
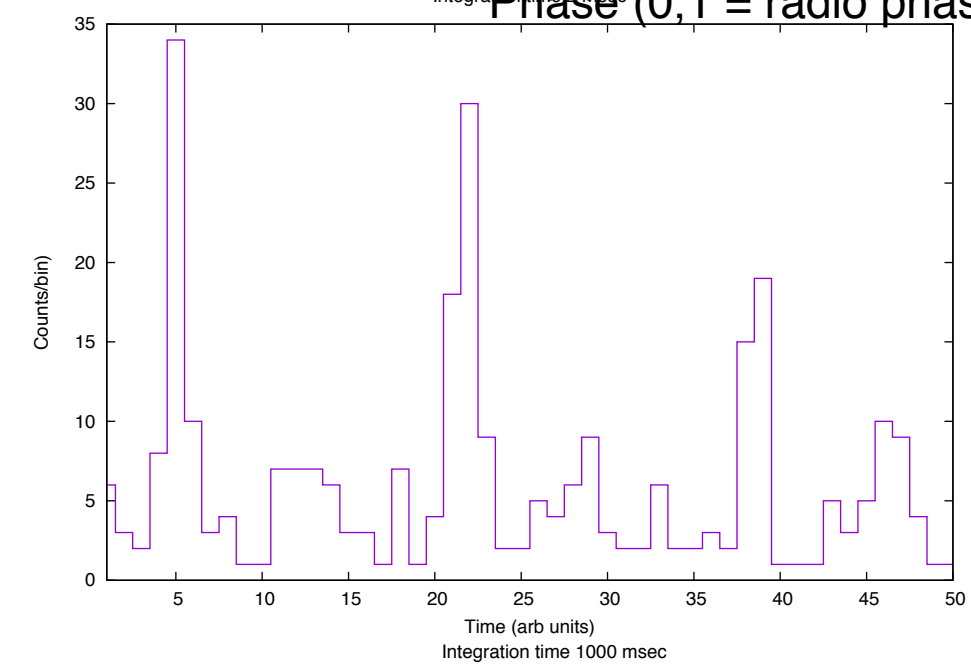
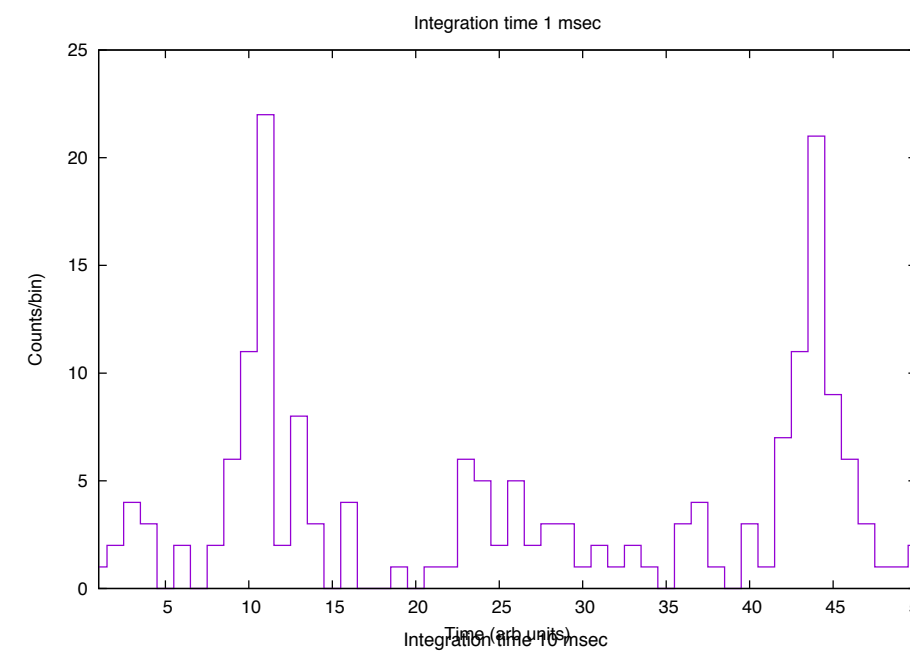
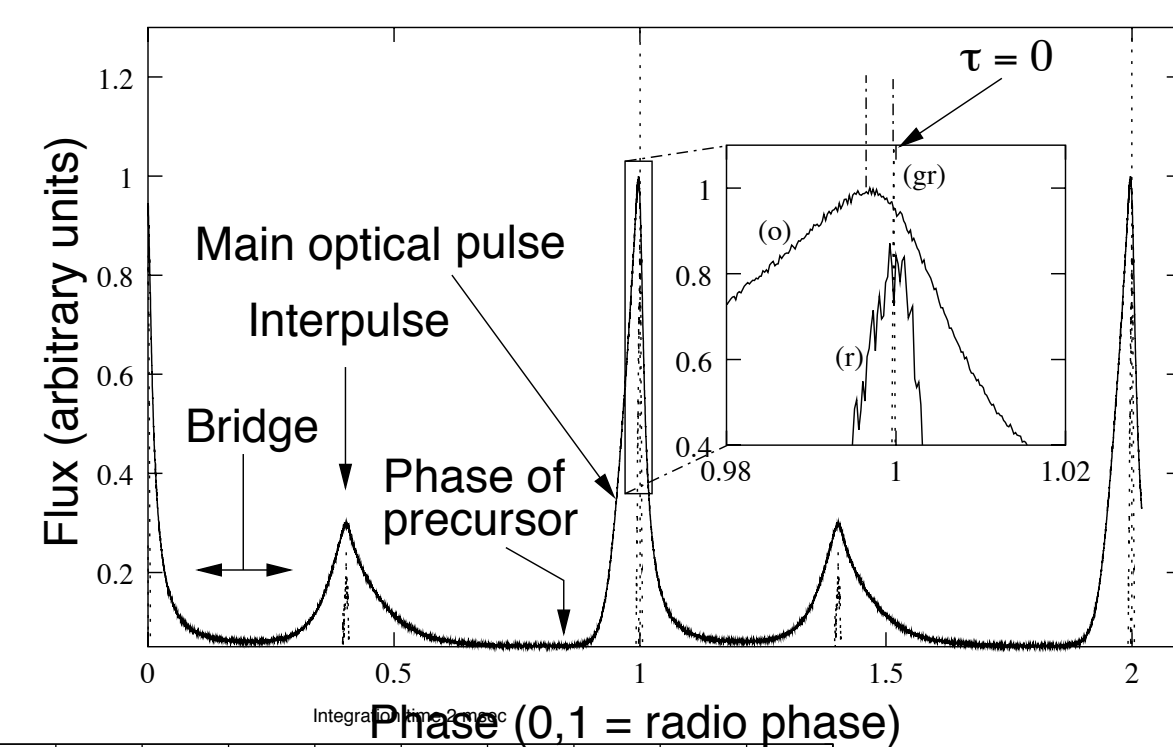
NUI Galway
OÉ Gaillimh



Pulsar : optical spectra



Pulsars : what happens if we don't have good timing



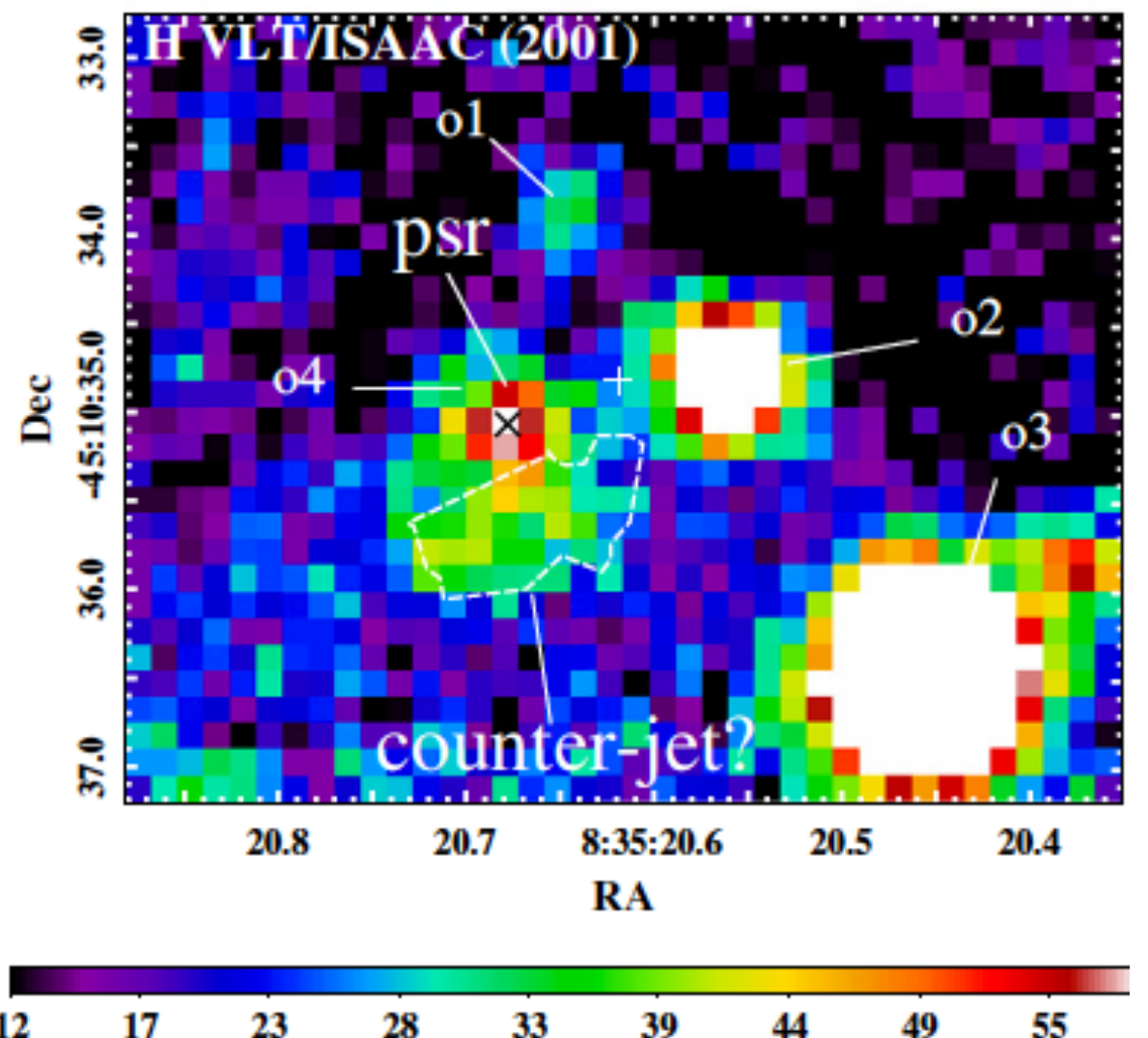


Figure 1. $5''.5 \times 4''.5$ fragment of the Vela pulsar vicinity as seen with the VI and nearby field objects are marked using notations from Shibanov et al. (2013). A seven-pixel Gaussian kernel to better underline the morphology of the extended feature in the right frame indicates the projection of the X-ray counter-jet axis on the sky. The left and Gemini (2013) observations, respectively. The long and short arrows indicate the direction of the extended feature, respectively. The polygon is the aperture used for the photometric analysis.

Vela : K Band



NUI Galway
OÉ Gaillimh

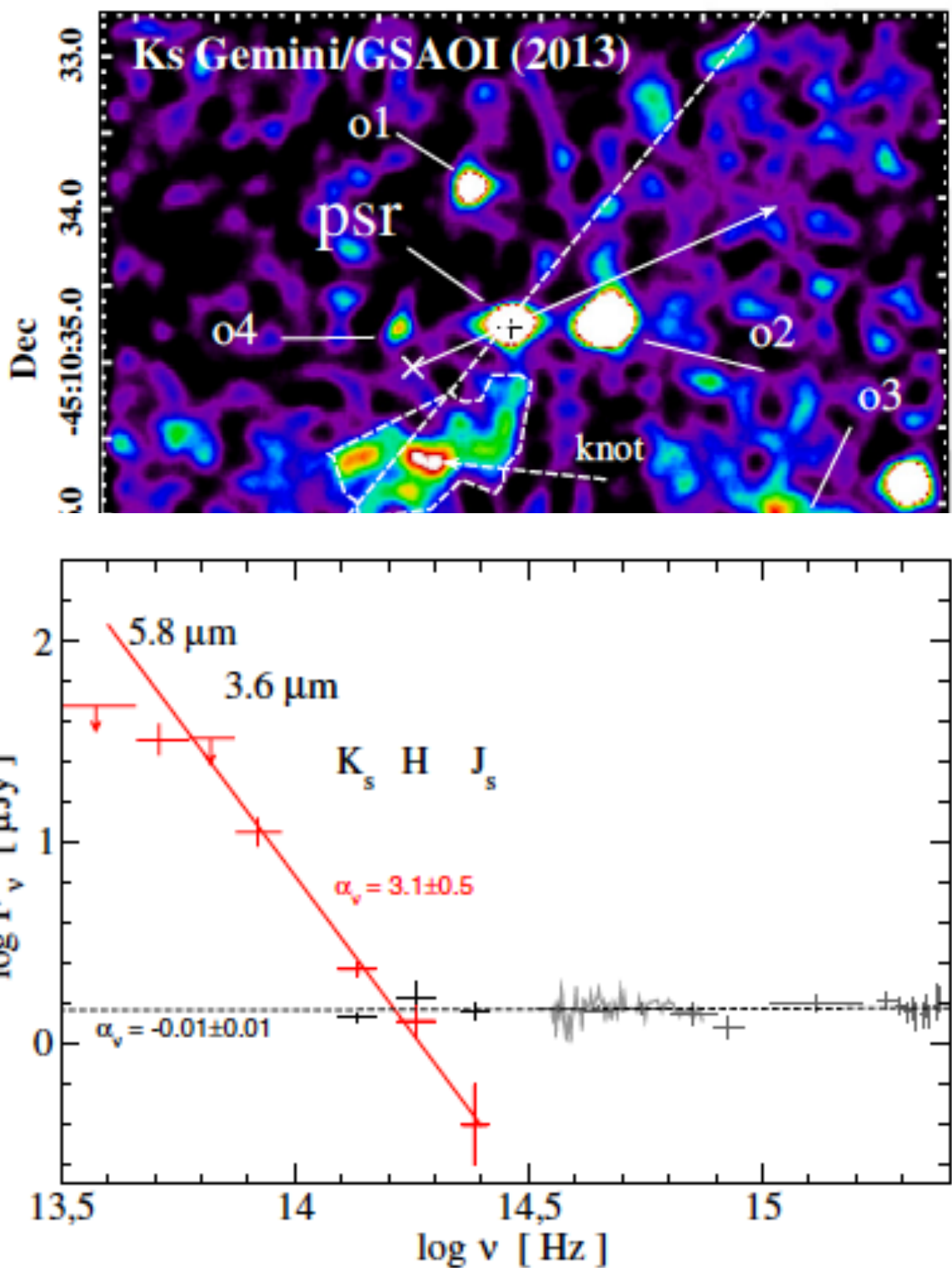
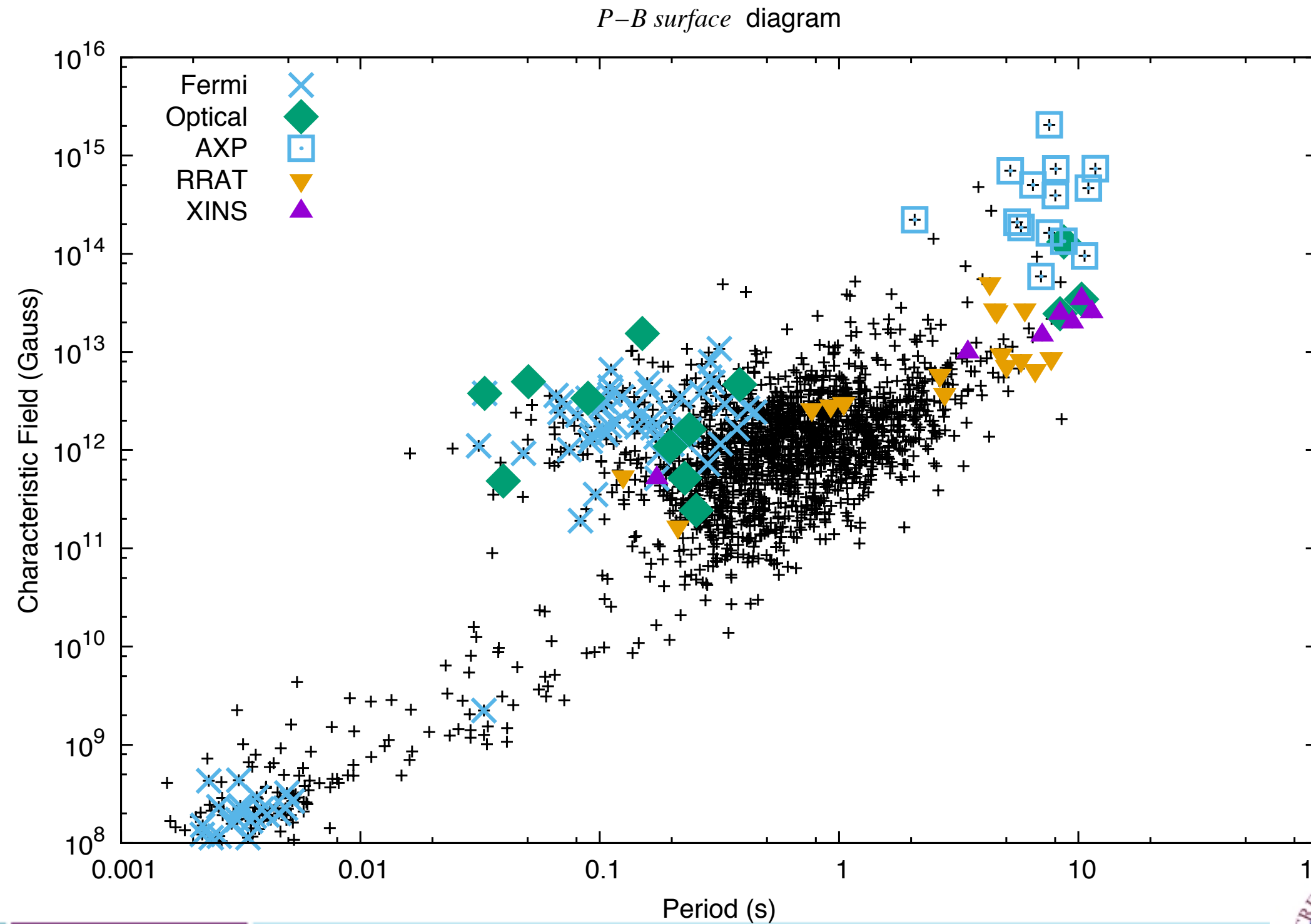


Figure 2. IR–UV spectra of the Vela pulsar (black/gray) and the likely counter-jet feature (red). The UV–optical data are from Romani et al. (2005) and Mignani et al. (2007) and the IR data are from Shibanov et al. (2003) and Danilenko et al. (2011). The dashed line approximates the flat UV–optical spectrum of the pulsar. The red line is the best fit to the near-IR fluxes of the counter-jet. The index α_ν is defined as $F_\nu \propto \nu^{-\alpha_\nu}$.

Pulsar P - Surface Field



NUI Galway
OÉ Gaillimh

Erice 11th October 2015



Anomalous X-ray Pulsars / Magnetars

Name	P (s)	Bsurf (10^{14} G)	dE/dt (10^{33} erg/s)	Lx{b} (10^{33} erg/s)	Opt (K mag)
1E 2259+586	6.979	0.59	0.056	17	21.4
Swift J1822.3-1606	8.438	0.14	0.0014	0.005	
1E 1048.1-5937	6.458	3.9	3.3	49	20.5
1E 1841-045	11.789	7	0.99	184	
4U 0142+61	8.689	1.3	0.12	105	20
SGR 1806-20	7.548	20	45	163	20
SGR 1900+14	5.200	7	26	90	
SGR 0501+4516	5.762	1.9	1.2	0.81	19
1E 1547.0-5408	2.072	3.2	210	1.3	
XTE J1810-197	5.540	2.1	1.8	0.043	21
CXOU J010043.1-721134	8.020	3.9	1.4	65	
SGR 0418+5729	9.078	0.061	0.00021	0.001	
SGR 0526-66	8.054	5.6	2.9	189	
PSR J1622-4950	4.326	2.7	8.3	0.44	
SGR 1627-41	2.595	2.2	43	3.6	
1RXS J170849.0-400910	11.005	4.7	0.58	42	
CXOU J171405.7-381031	3.825	5	45	56	
SGR J1745-2900	3.764	2.3	10	<0.11	
SGR 1833-0832	7.565	1.6	0.32	...	
PSR J1846-0258‡	0.327	0.49	8100	19	
SGR 1935+2154†	3.245	



NUI Galway
OÉ Gaillimh

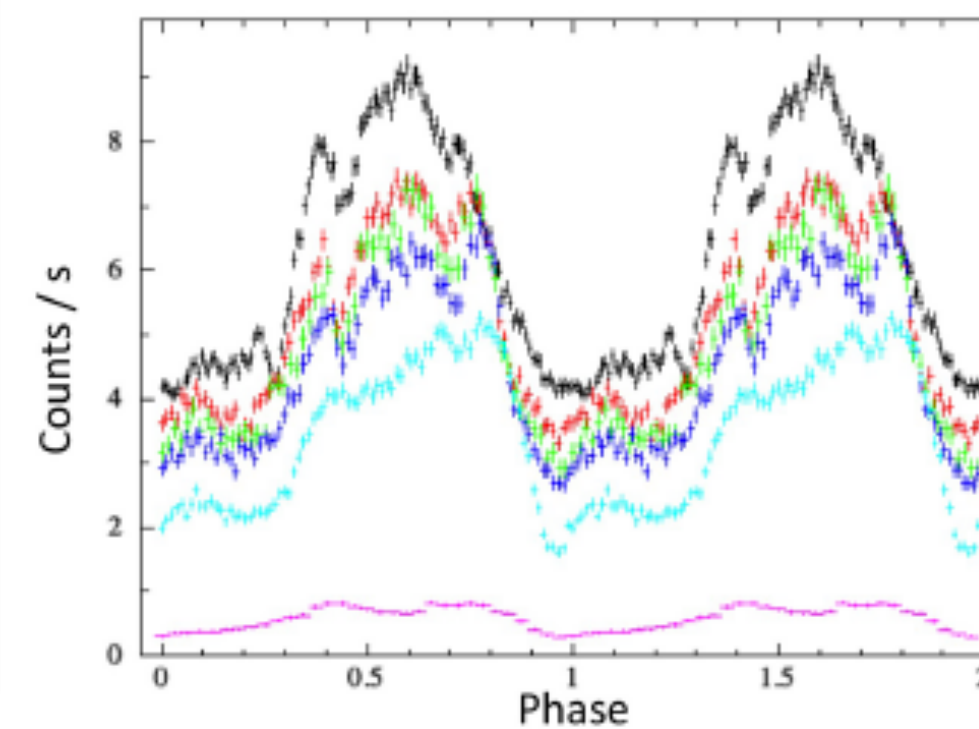
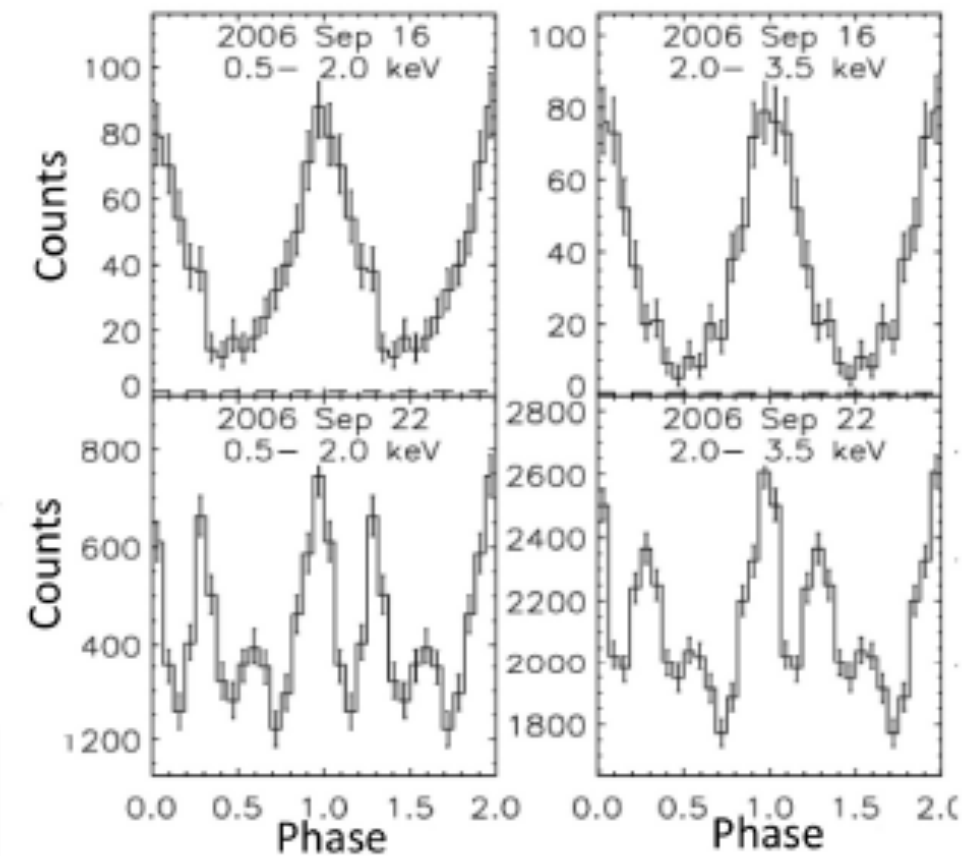
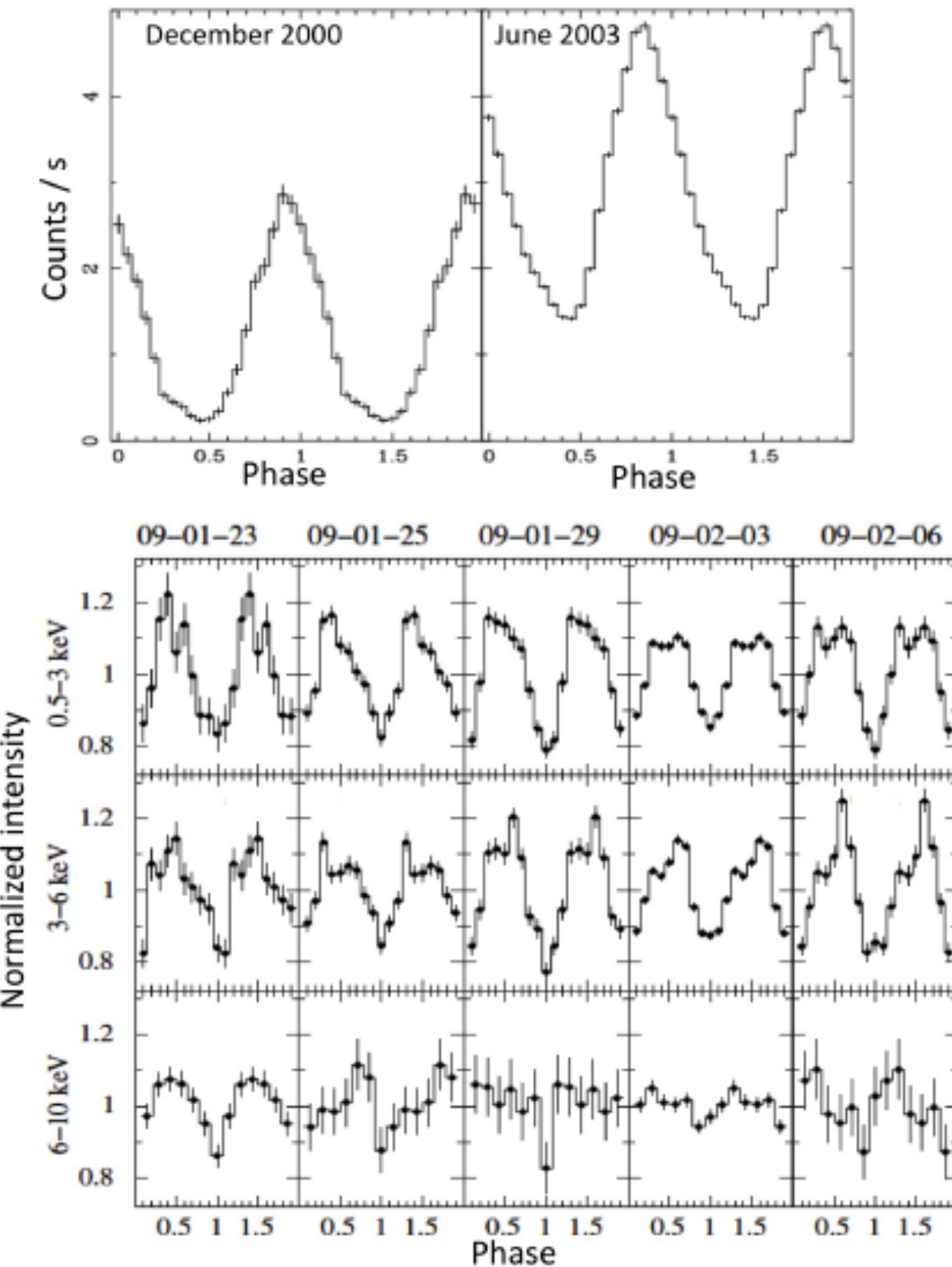


ETTORE MAJORANA FOUNDATION AND
CENTRE FOR SCIENTIFIC CULTURE

TO PAY A PERMANENT TRIBUTE TO GALILEO GALILEI, FOUNDER OF MODERN SCIENCE
AND TO ENRICO FERMI, "THE ITALIAN NAVIGATOR", FATHER OF THE WEAK FORCES

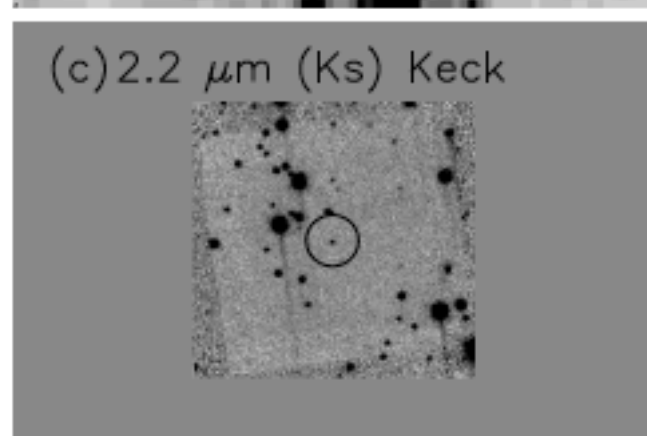
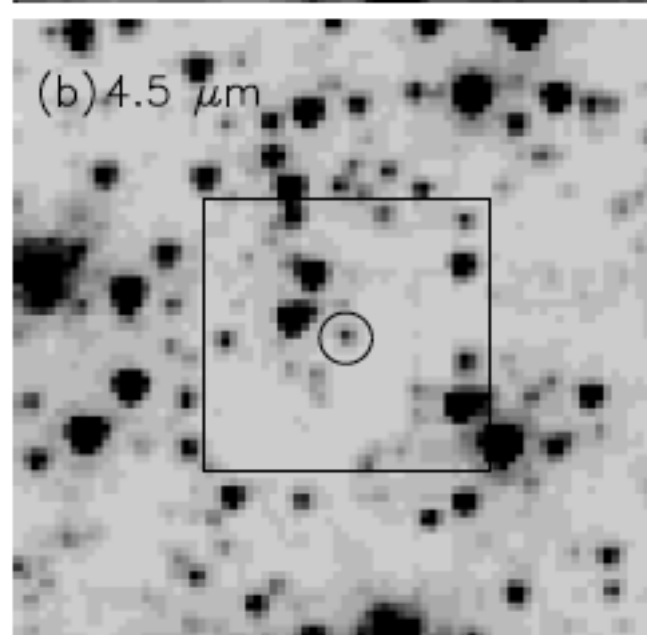
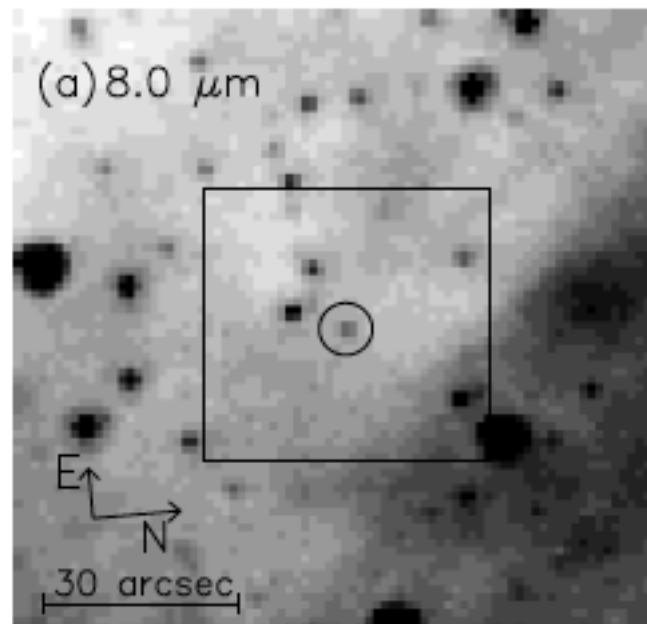


Review - Mereghetti, Pons and Metallos : arXiv:1503.06313v1 : X-ray observations

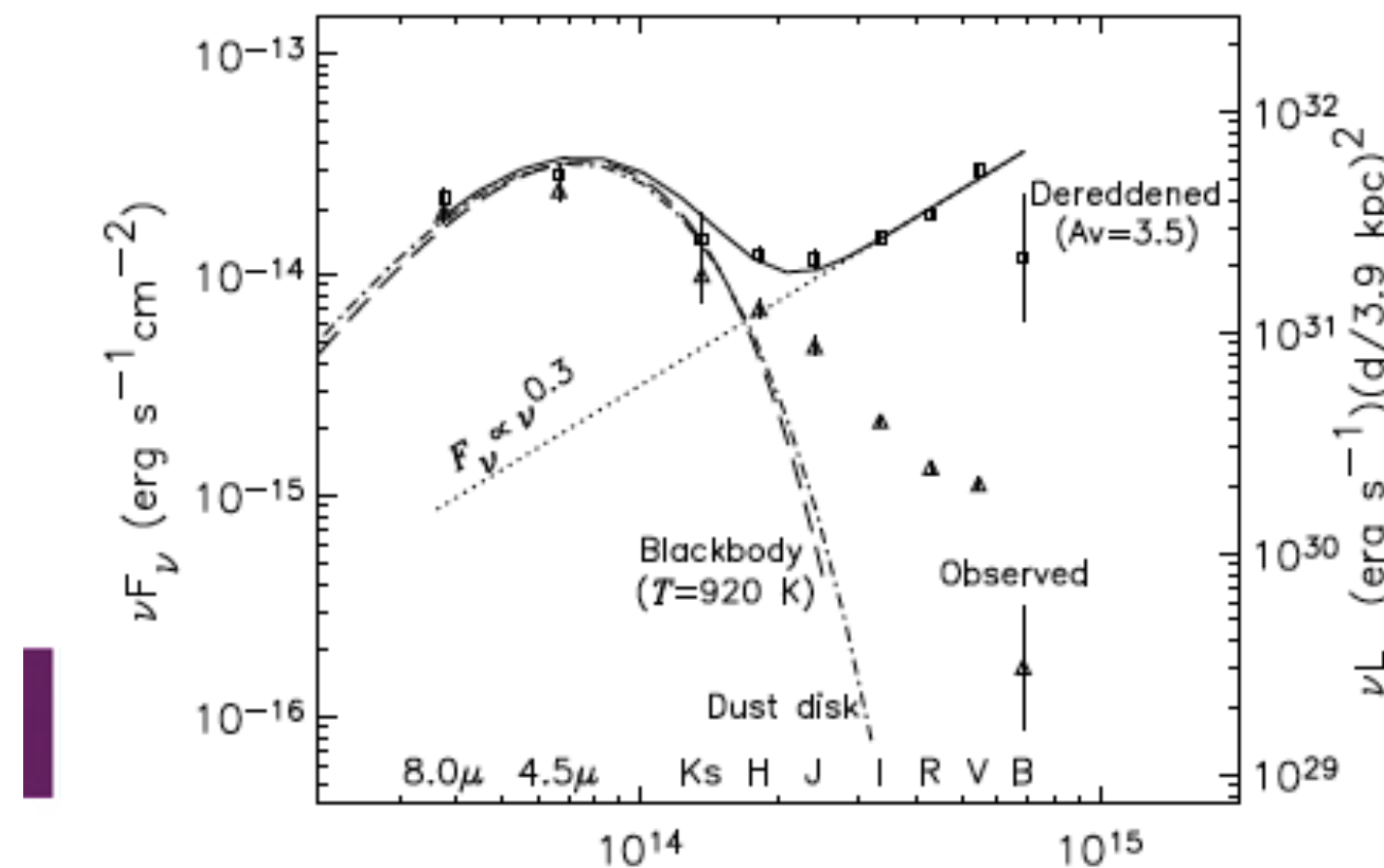


Optical/NIR Magnetars

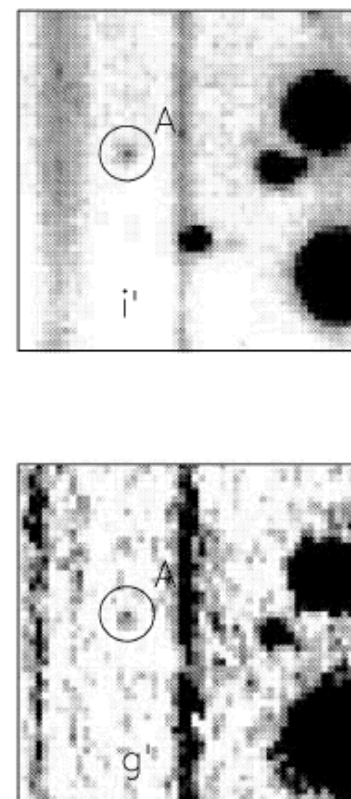
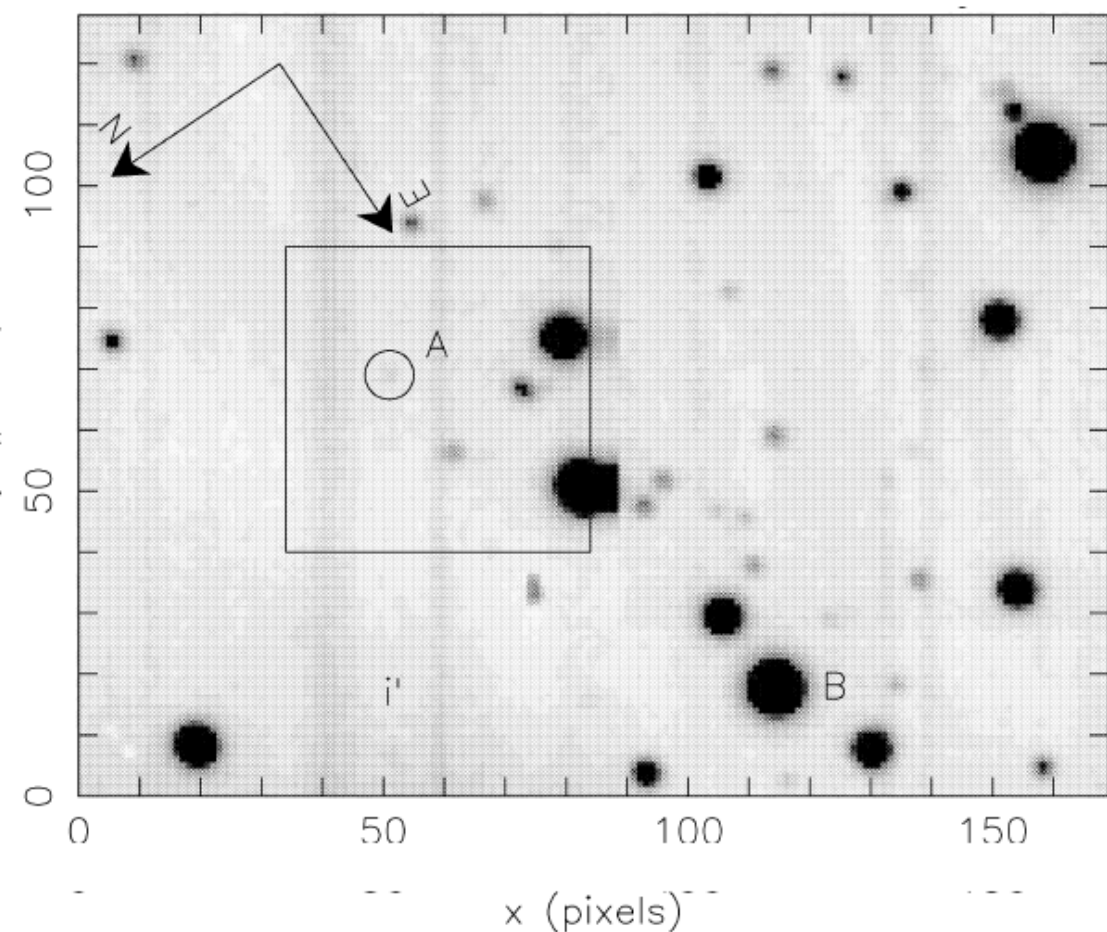
4U 01642+61 : Wang et al, 2006, Nature, 440, 772



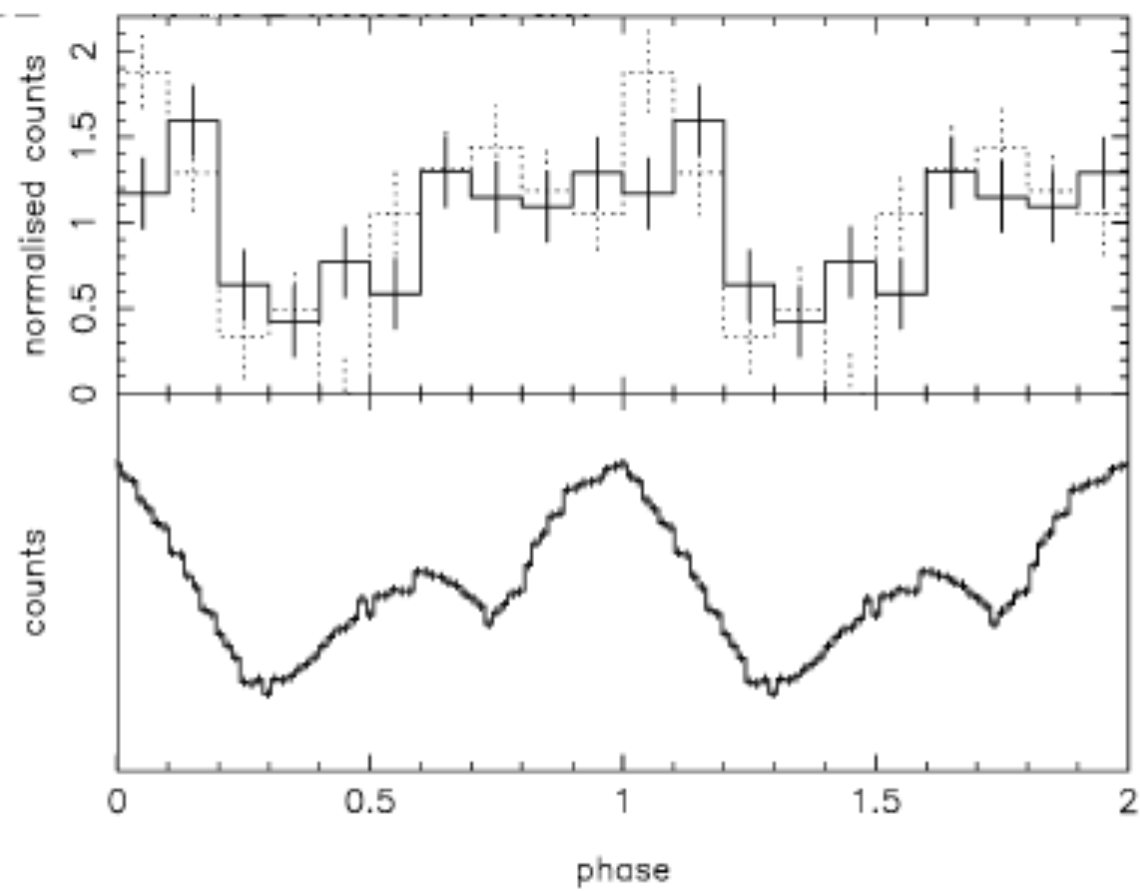
Name	Year	Age	mag	D(kpc)	A_V	Phot
SGR1806-20	2004	3.14	20.1	15	29	IR
1E 1547.0-5408	2009	3.14	18.5	9	17	IR
1E 1048.1-5937	2004	3.63	21.3	3	6.1	OIR
XTE J1810-197	2004	3.75	20.8	4	5.1	IR
SGR 0501+4516	2009	4.1	19.1	~2	5	IR
4U 0142+61	2002	4.84	20.1	>5	5.1	OIR
1E 2259+586	2002	5.34	21.7	3	5.7	IR



4U0142+61 : Dhillon et al, 2005, MNRAS, 363, 609



31,000 frames of (0.48s)



NUI Galway
OÉ Gaillimh



SGR 0501+4516: Dhillon et al, 2011, MNRAS. 416. L16

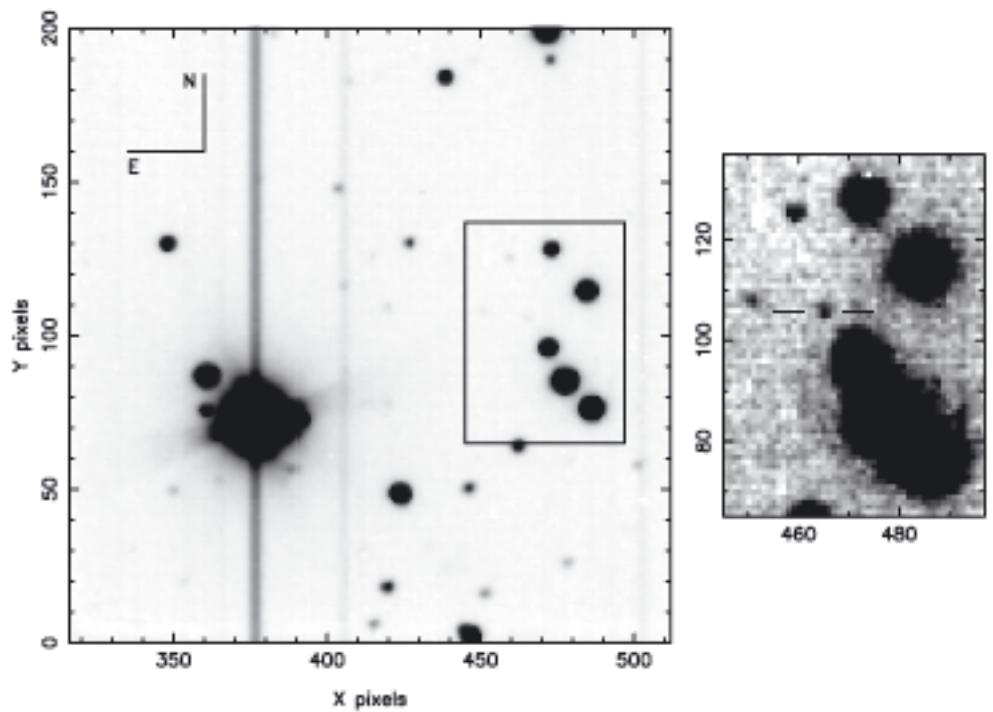


Figure 1. i' -band finding chart for SGR 0501+4516. Left-hand panel: summed i' -band image of the field around SGR 0501+4516 on 2009 January 1, with a total exposure time of 3247 s. The box (inset) shows the portion of the field that is plotted at a higher contrast in the right-hand panel. The orientation of the image is marked on the upper left-hand side of the left-hand panel. The pixel scale is $0.3 \text{ arcsec pixel}^{-1}$; hence, the field of view in this image is $60 \times 60 \text{ arcsec}^2$. The vertical streaks are due to the frame-transfer process. Right-hand panel: higher-contrast plot of a $16 \times 22 \text{ arcsec}^2$ field around SGR 0501+4516, highlighting the detection of the pulsar in the i' band. The X-ray error circle lies within the seeing disc of the pulsar and is hence invisible.

K band - on NIRI/Gemini
but very poor absolute timing

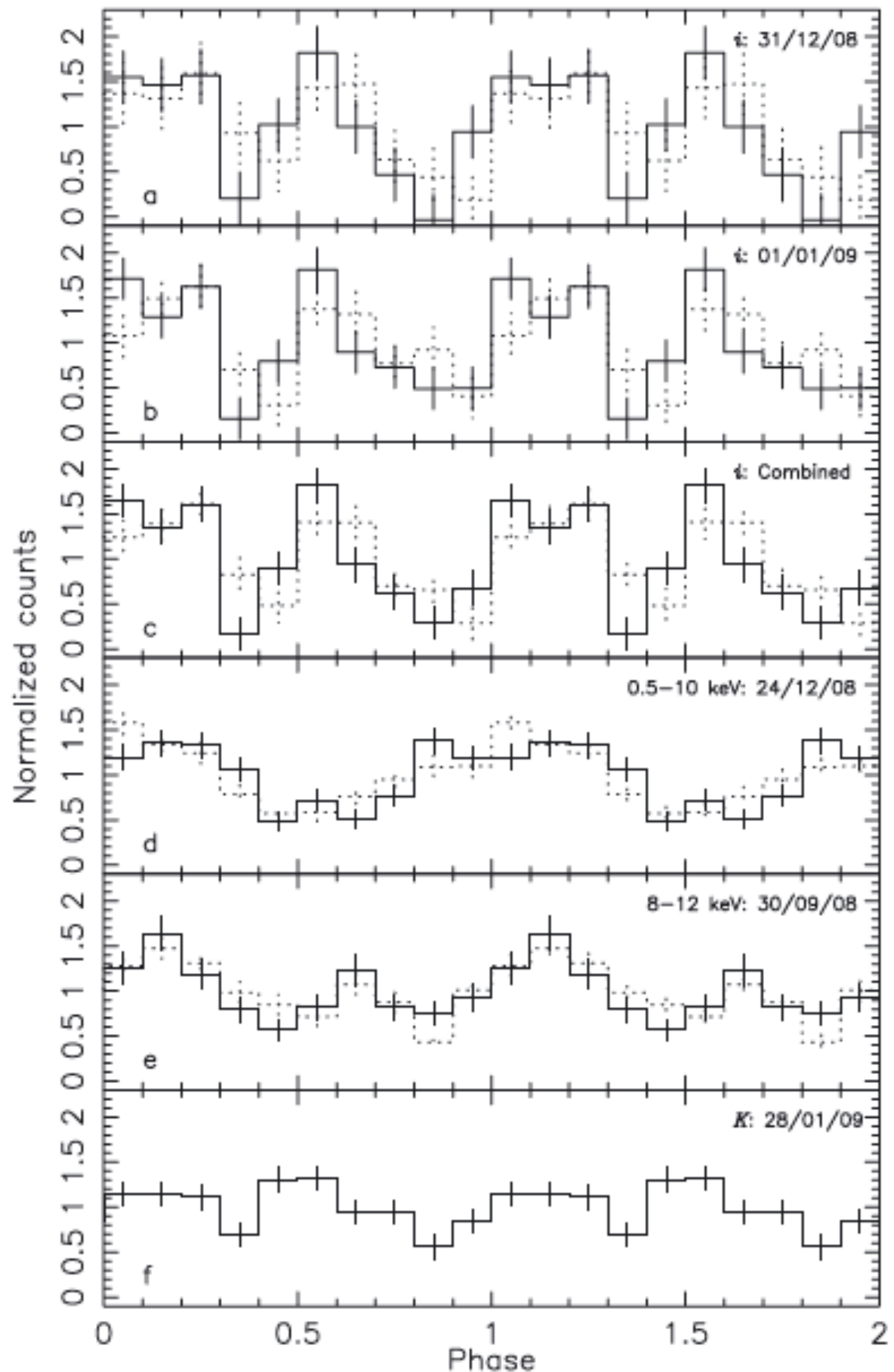


NUI Galway
OÉ Gaillimh



ETTORE MAJORANA FOUNDATION AND
CENTRE FOR SCIENTIFIC CULTURE

TO PAY A PERMANENT TRIBUTE TO GALILEO GALILEI, FOUNDER OF MODERN SCIENCE
AND TO ENRICO FERMI, "THE ITALIAN NAVIGATOR", FATHER OF THE WEAK FORCE



1E 1048.1-5937

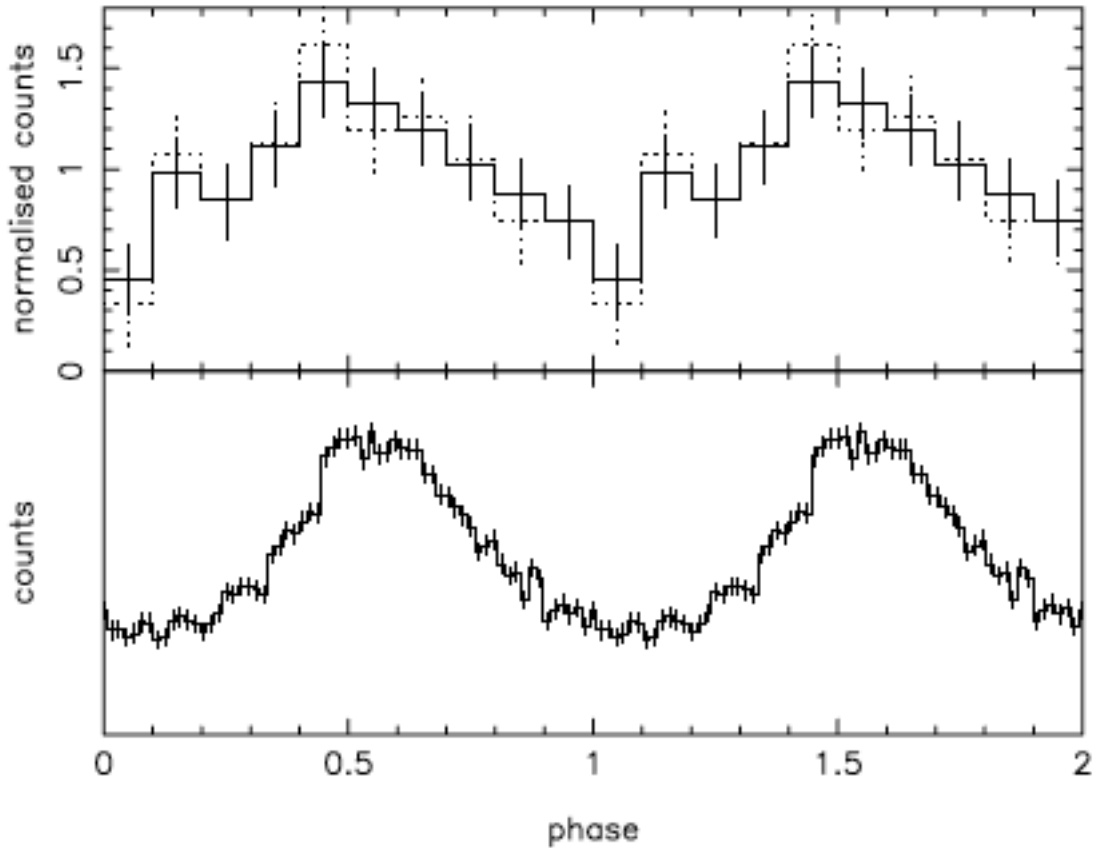


Figure 2. Top: the solid and dotted lines show optical pulse profiles of 1E 1048.1–5937 in the i' band obtained using techniques (i) and (ii), respectively (see Sections 2.1 and 2.2). Each pulse profile was first corrected for transparency variations using the comparison star shown in Fig. 1, although the correction made only a negligible difference to the light curves. The pulse profiles were then normalized by dividing by the mean number of counts. For clarity, two cycles are shown. Bottom: averaged X-ray pulse profile of 1E 1048.1–5937 in the 2–10 keV energy band spanning the epoch of the optical observations (Dib et al. 2009). Note that it is not possible to estimate the X-ray pulsed fraction from this profile as the PCA on *RXTE* has a 1° field of view and no imaging capability, rendering the background level uncertain. For this reason, no scale is given on the ordinate.

Dhillon et al, 2009, MNRAS, 394, L112

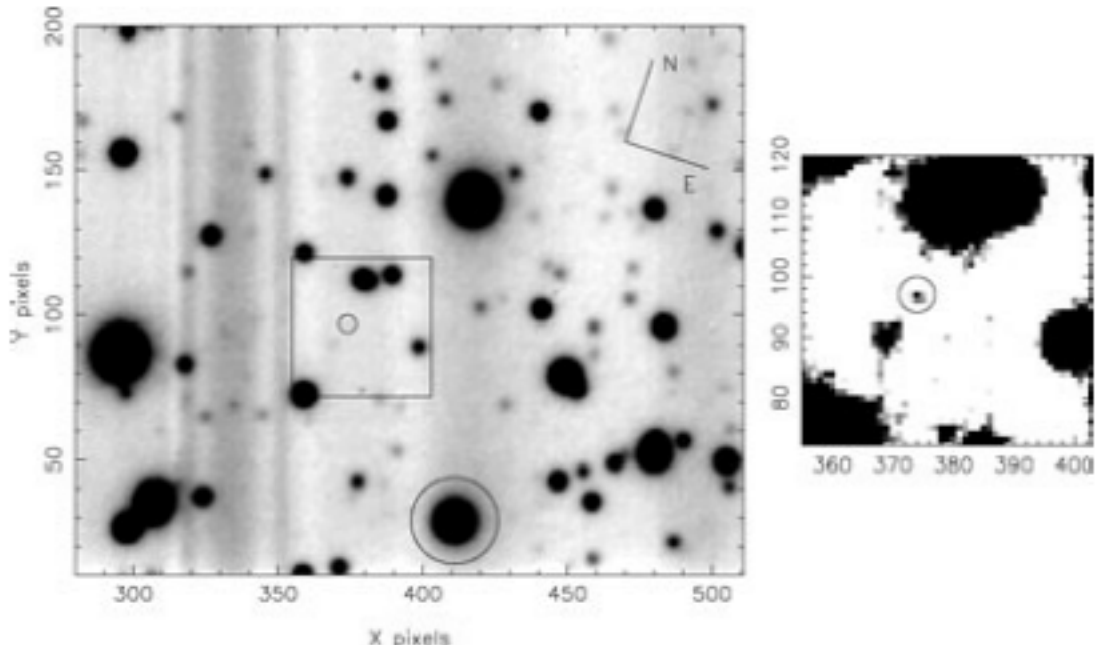


Figure 1. Left-hand side: summed i' -band image of the field around 1E 1048.1–5937, with a total exposure time of 10 684 s. For clarity, only a portion of one of the two ULTRACAM windows is shown. The positions of 1E 1048.1–5937 and the comparison star are indicated by circles near the centre and bottom of the image, respectively. The central box shows the portion of the field that is plotted at a higher contrast on the right-hand side. The orientation of the image is marked on the upper right-hand side. The pixel scale is $0.156 \text{ arcsec pixel}^{-1}$, hence the field of view in this image is $36 \times 30 \text{ arcsec}^2$. The vertical banding is due to residual bias structure. Right-hand side: higher contrast plot of a $7.5 \times 7.5 \text{ arcsec}^2$ field around 1E 1048.1–5937, highlighting the detection of the pulsar in the i' band.



NUI Galway
OÉ Gaillimh



ETTORE MAJORANA FOUNDATION AND
CENTRE FOR SCIENTIFIC CULTURE

TO PAY A PERMANENT TRIBUTE TO GALILEO GALILEI, FOUNDER OF MODERN SCIENCE
AND TO ENRICO FERMI, "THE ITALIAN NAVIGATOR", FATHER OF THE WEAK FORCES



Anomalous X-ray Pulsars / Magnetars

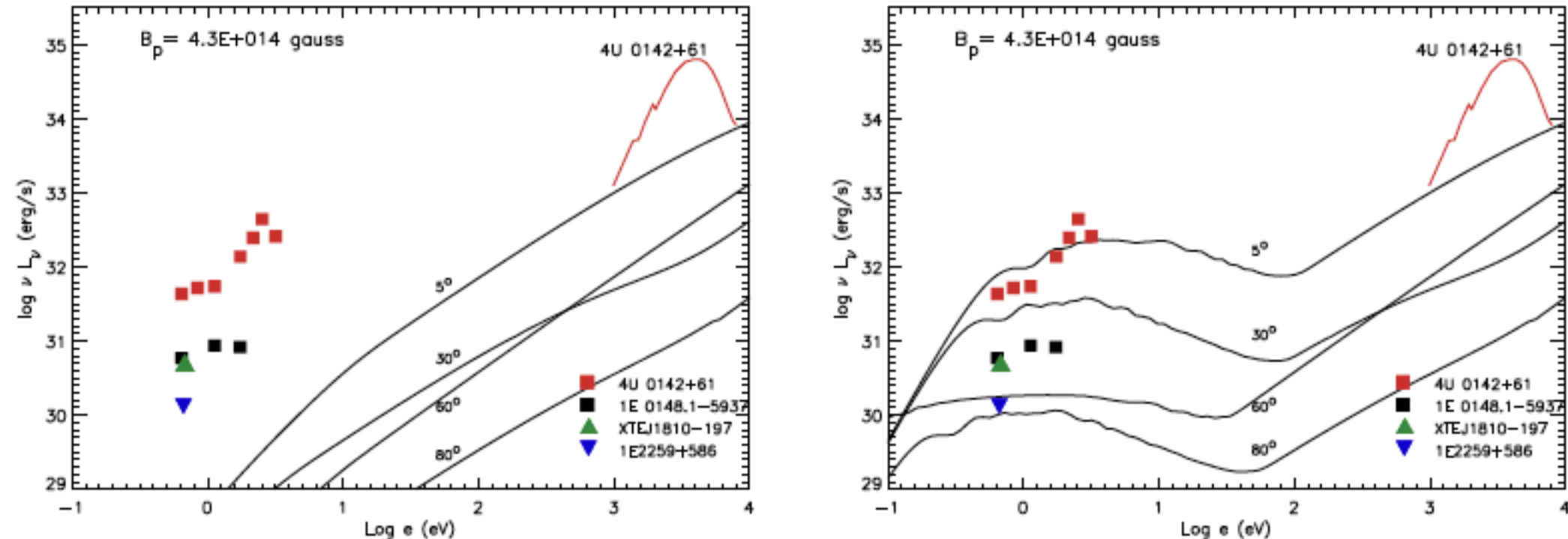


Fig. 2 Model spectra for different values of θ_{obs} and $B_p = 4.3 \times 10^{14}$ G. The *XMM-Newton* X-ray spectrum of 1RXS J1708-4009 is from Rea et al. (2008; red solid line). The AXPs IR/optical data are from Duncan & van Kerkwijk 2005 (4U 0142+614 and 1E 1048-5937) and Mignani et al. 2007 (XTE J1810-197 and 1E 2259+586). The adopted distances for de-reddening are 5 kpc (4U 0142+614, 1RXS J1708-4009), 3 kpc (1E 1048-5937, 1E 2259+586), 4 kpc (XTE J1810-197), 8.5 kpc (1E 1841-045). *Left:* Spectra computed for incoherent curvature emission. *Right:* Same as in the left panel, but accounting for particle bunching.



NUI Galway
OÉ Gaillimh



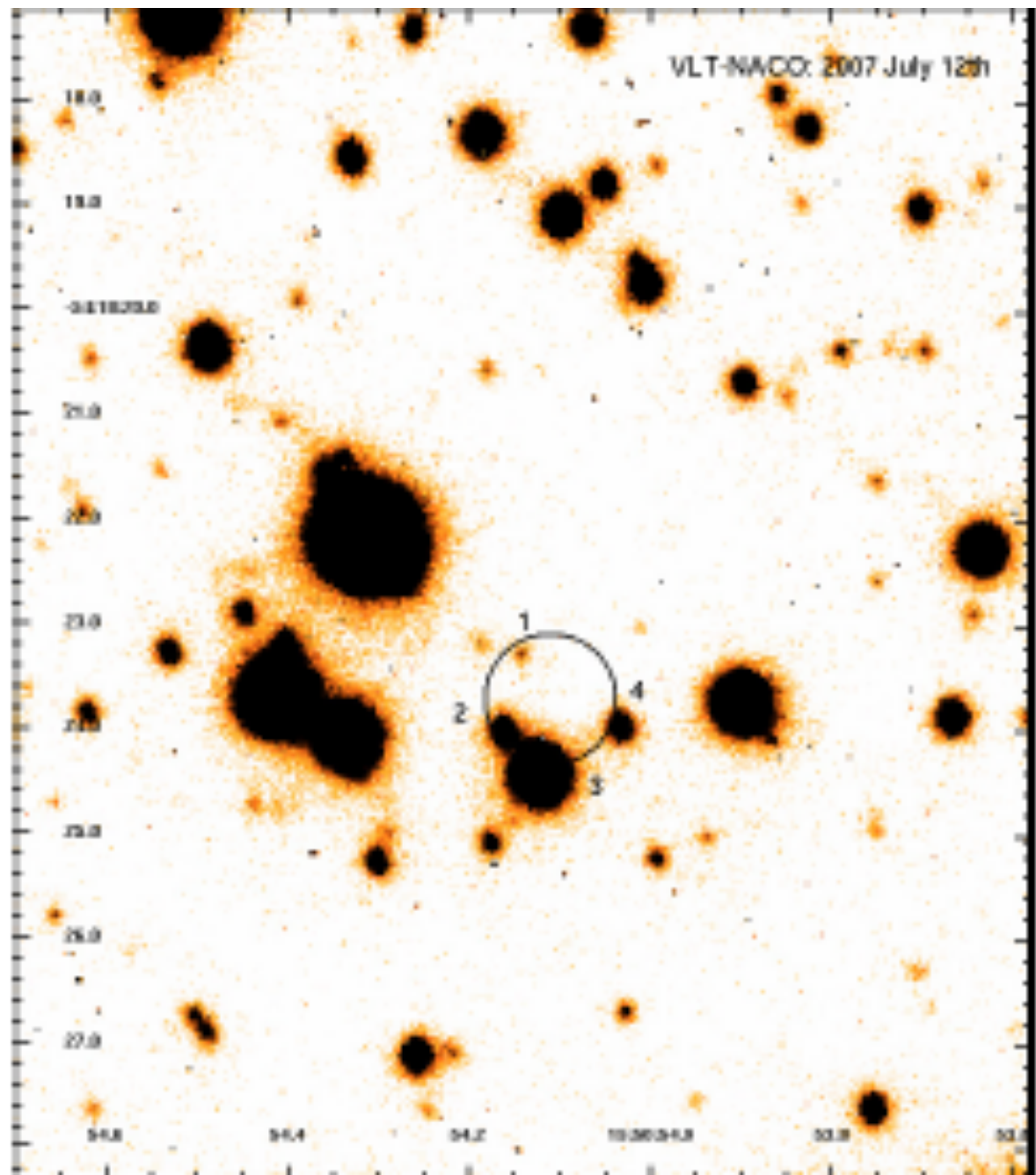
AO Observations of a Magnetar - VLT/NACO : Mignani et al., 2009, A&A, 497, 451

Source ID	Δr	2007-07-08	2007-07-12
1	0'.50	≥ 20.1	20.27 ± 0.05
2	0'.54	18.65 ± 0.08	18.51 ± 0.03
3	0'.76	16.22 ± 0.05	16.23 ± 0.03
4	0'.74	18.56 ± 0.06	18.54 ± 0.03

Table 1. Log of the *VLT/NACO* K_s -band observations of the 1E 1547.0–5408 field.

Epoch (yyyy-mm-dd)	MJD	Exp. time (s)	Seeing (")	Airmass
2007-07-08	54 289	1440	1.18	1.16
2007-07-12	54 293	1440	0.55	1.17
2007-08-17	54 329	1800	1.60	1.19

Columns report the observing epoch and Modified Julian Date (MJD), the total exposure time $T = \text{DIT} \times \text{NDIT} \times N$, where N is the number of nodes of the dithering pattern, and the average seeing and airmass during the observations.



NUI Galway
OÉ Gaillimh

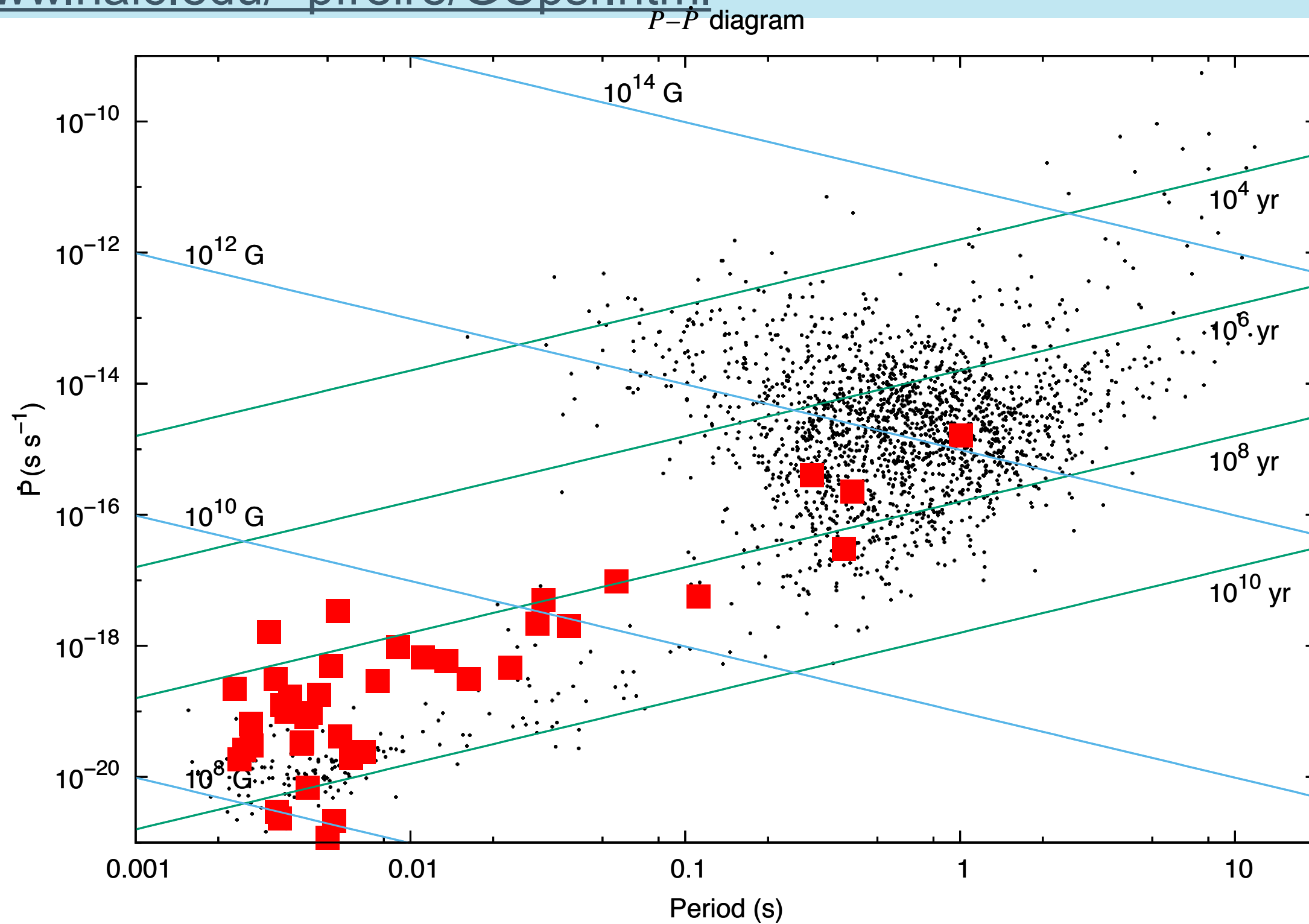


ETTORE MAJORANA FOUNDATION AND
CENTRE FOR SCIENTIFIC CULTURE

TO PAY A PERMANENT TRIBUTE TO GALILEO GALILEI, FOUNDER OF MODERN SCIENCE
AND TO ENRICO FERMI, "THE ITALIAN NAVIGATOR", FATHER OF THE WEAK FORCES



Millisecond Pulsars - see (e.g.) Paulo Freire's page <http://www.naic.edu/~pfreire/GCpsr.html>



NUI Galway
OÉ Gaillimh

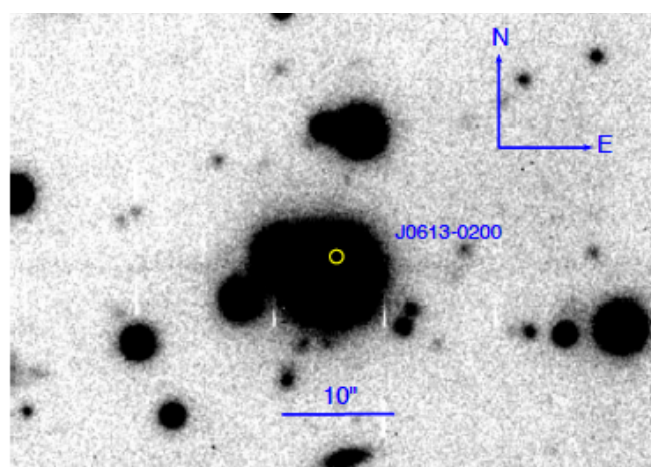


Radio discovery parameters field MSP

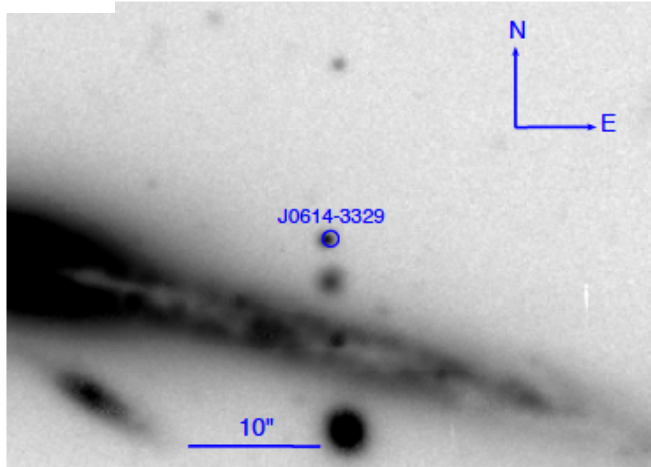
Pulsar	P_b (d)	e	M_C (M_\odot)	Class.	Refs.
J0613–0200	1.198	0.0000055	0.13	He WD	Verbiest et al. (2009)
J0614–3329	53.584	0.0001801	0.28	WD	Ransom et al. (2011)
J1231–1411	1.860	0.000004	0.19	WD	Ransom et al. (2011)
J2017+0603	2.198	0.0000005	0.18	He WD	Cognard et al. (2011)

PSR	α (hms)	δ ($^{\circ} \ ' \ ''$)	Δr	g	r	i
J0614–3329	06 14 10.333	−33 29 54.19	0''.19	21.95±0.05	21.70±0.03	21.58±0.03
J1231–1411	12 31 11.299	−14 11 43.39	0''.31	25.40±0.23	23.95±0.06	23.35±0.11
J2017+0603	20 17 22.714	+06 03 05.82	0''.29	24.72±0.28	24.06±0.25	23.84±0.17

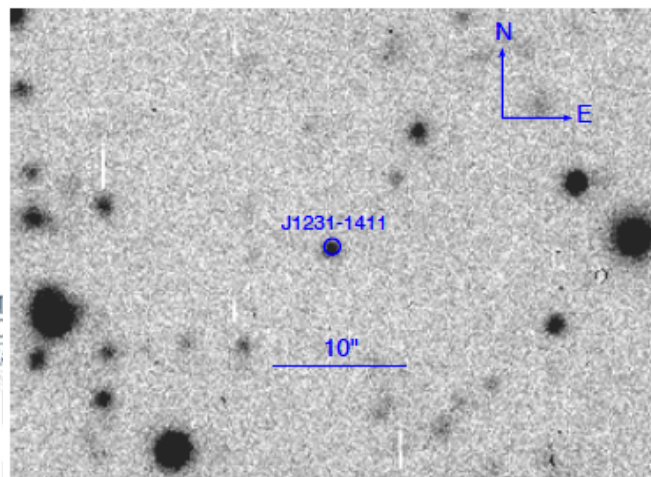
Follow up optical spectroscopy needed



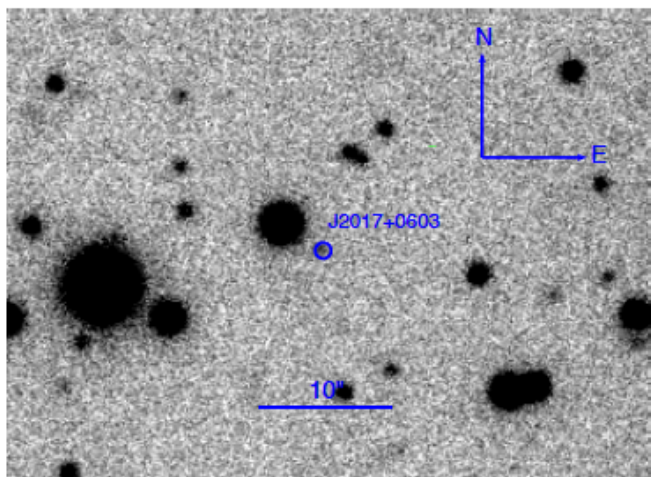
(a) J0613–0200



(b) J0614–3329



(c) J1231–1411



(d) J2017+0603

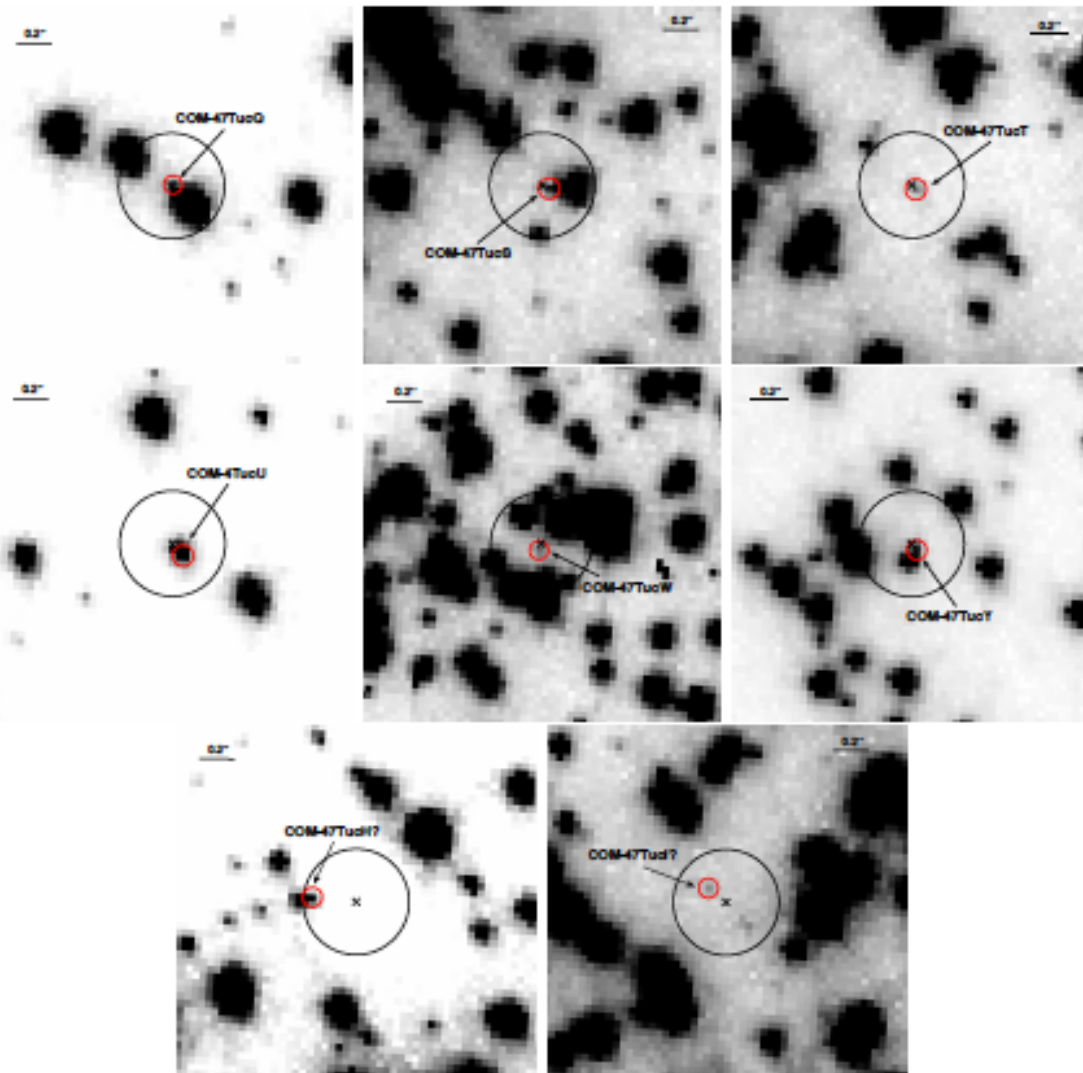


NUI Galway
OÉ Gaillimh



Millisecond Pulsars

- Cadelano, et al, 2015, ApJ, 812, 63



Name	α (h m s)	δ ($^{\circ}$ $'$ $''$)	dist ('")	m_{F300X}	m_{F390W}
COM-47TucQ	00 24 16.489	-72 04 25.209	0.04	23.19 ± 0.02	23.63 ± 0.05
COM-47TucS	00 24 3.977	-72 04 42.385	0.03	23.29 ± 0.02	23.80 ± 0.05
COM-47TucT	00 24 8.549	-72 04 38.965	0.04	23.07 ± 0.02	23.56 ± 0.03
COM-47TucU	00 24 9.835	-72 03 59.746	0.06	20.40 ± 0.01	20.85 ± 0.03
COM-47TucW	00 24 6.063	-72 04 49.133	0.06	24.28^a	23.62^a
COM-47TucY	00 24 1.401	-72 04 41.875	0.04	22.16 ± 0.02	22.69 ± 0.04
COM-47TucH?	00 24 6.755	-72 04 6.781	0.24	23.39 ± 0.02	24.25 ± 0.05
COM-47TucI?	00 24 7.953	-72 04 39.559	0.15	24.14 ± 0.04	22.43 ± 0.03

Table 3. Derived properties of the five MSPs with He WD companions

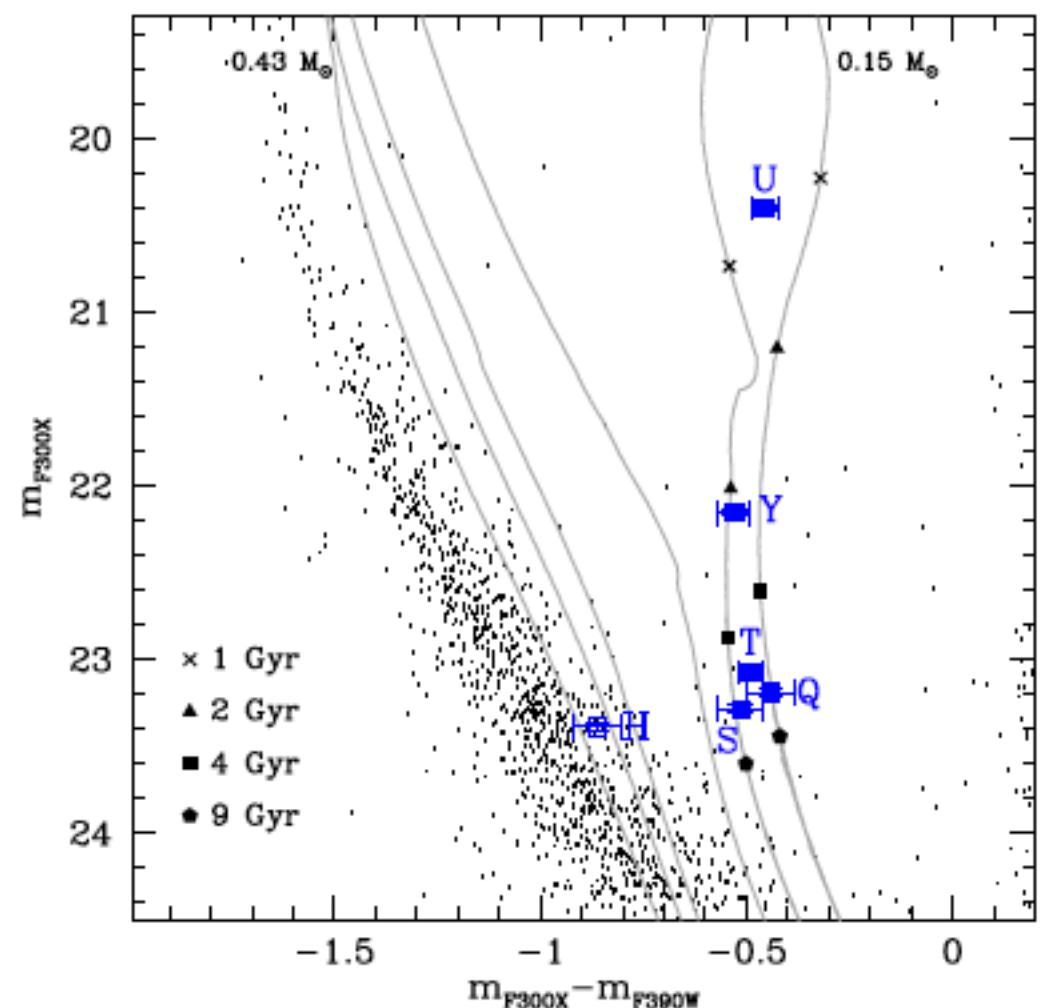
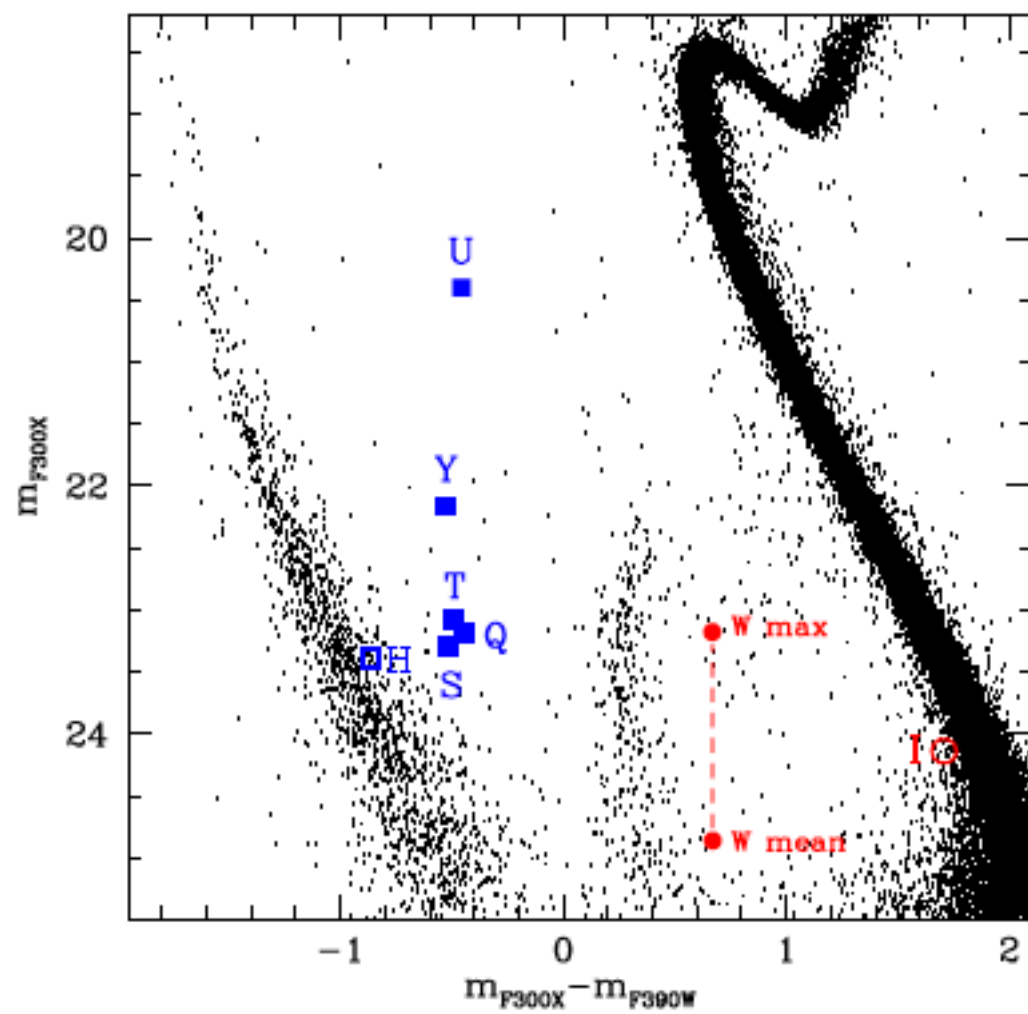
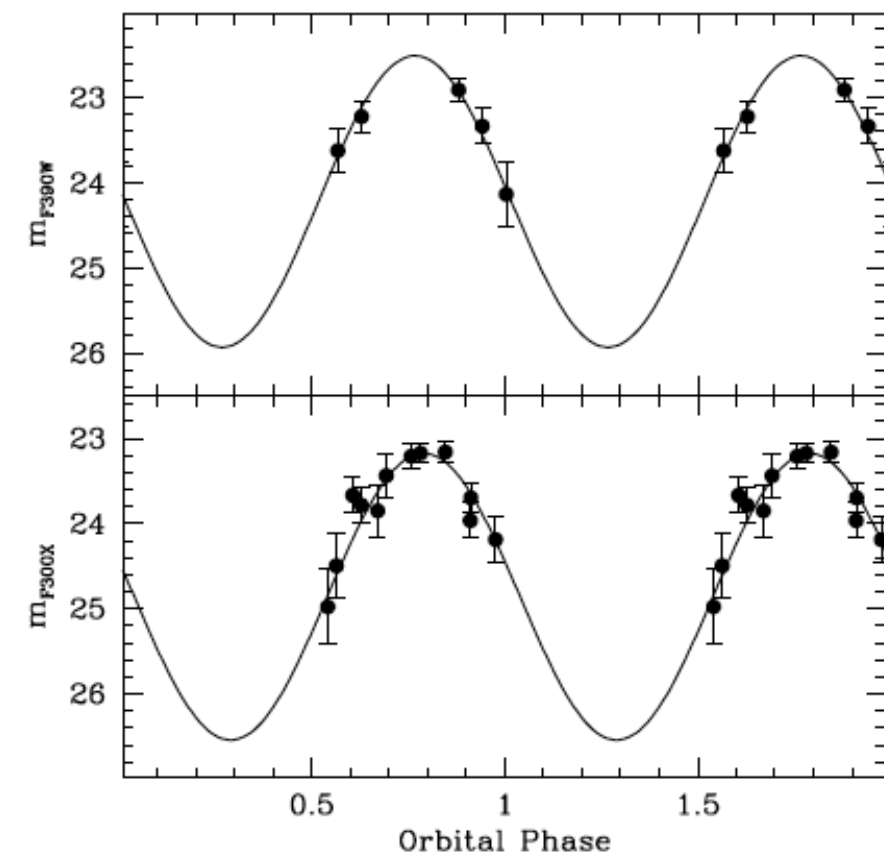
Parameter	47TucQ	47TucS	47TucT	47TucU	47TucY
M_{COM} (M_{\odot})	~ 0.15	$0.17^{+0.03}_{-0.02}$	$0.16^{+0.025}_{-0.01}$	$0.171^{+0.002}_{-0.003}$	0.17 ± 0.02
Age (Gyrs)	~ 5.5	$6.4^{+1.7}_{-6.0}$	$5.1^{+0.9}_{-3.5}$	$0.88^{+0.05}_{-0.06}$	$2.2^{+1.0}_{-1.6}$
T (10^3 K)	~ 7.6	$8.1^{+1.0}_{-0.7}$	$8.0^{+0.6}_{-0.5}$	$11.9^{+0.2}_{-0.5}$	$9.6^{+0.5}_{-1.2}$
L ($10^{-3} L_{\odot}$)	~ 9.5	$8.1^{+1.0}_{-0.3}$	$10.0^{+0.5}_{-0.6}$	158^{+7}_{-17}	23.0 ± 5
M_{PSR} (M_{\odot})	< 1.57	< 4.69	< 1.58	< 2.30	< 2.22
i ($^{\circ}$)	> 58	> 26	> 57	> 42	> 45



NUI Galway
OÉ Gaillimh

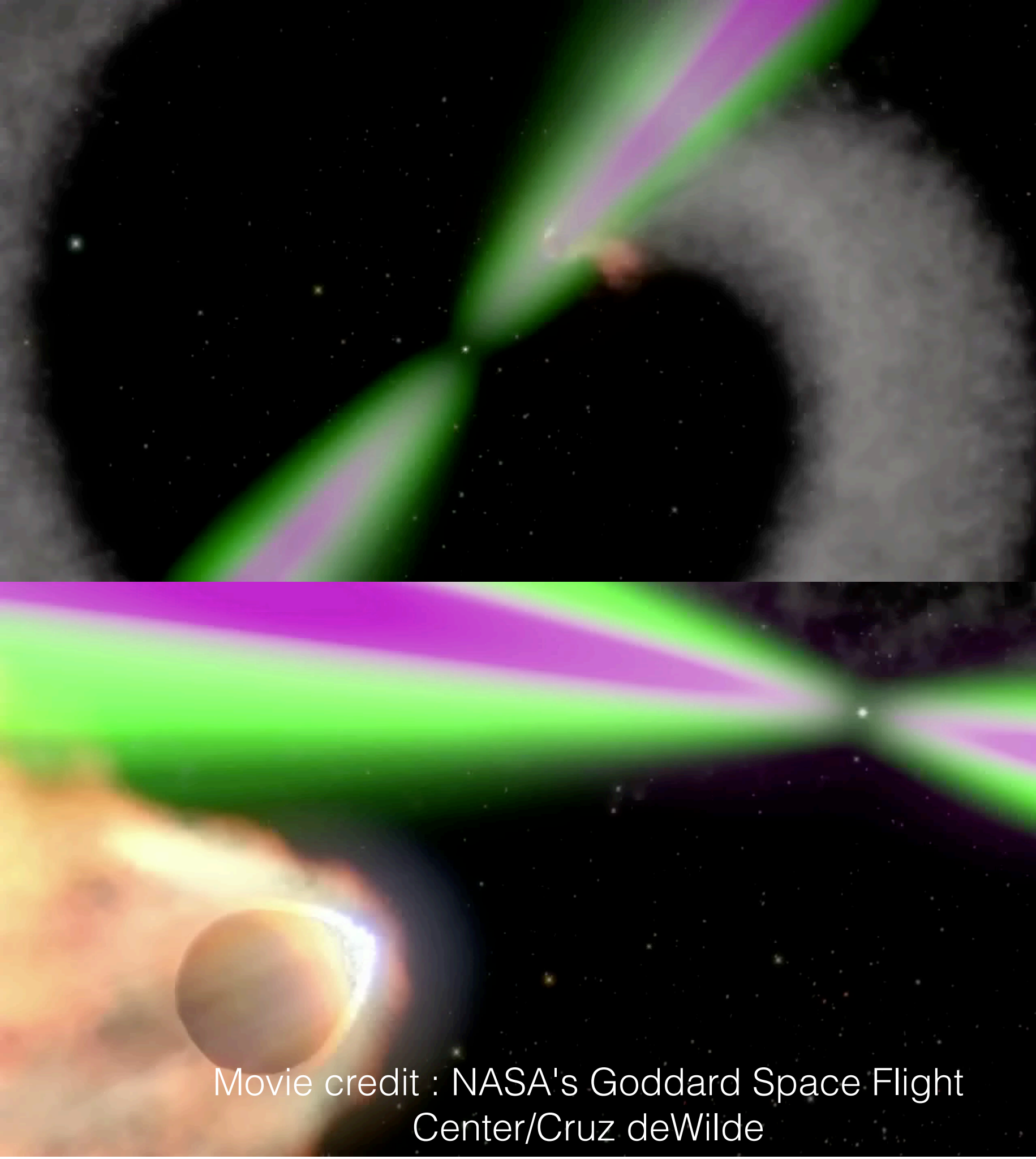


- Cadelano, et al, 2015, ApJ, 812, 63



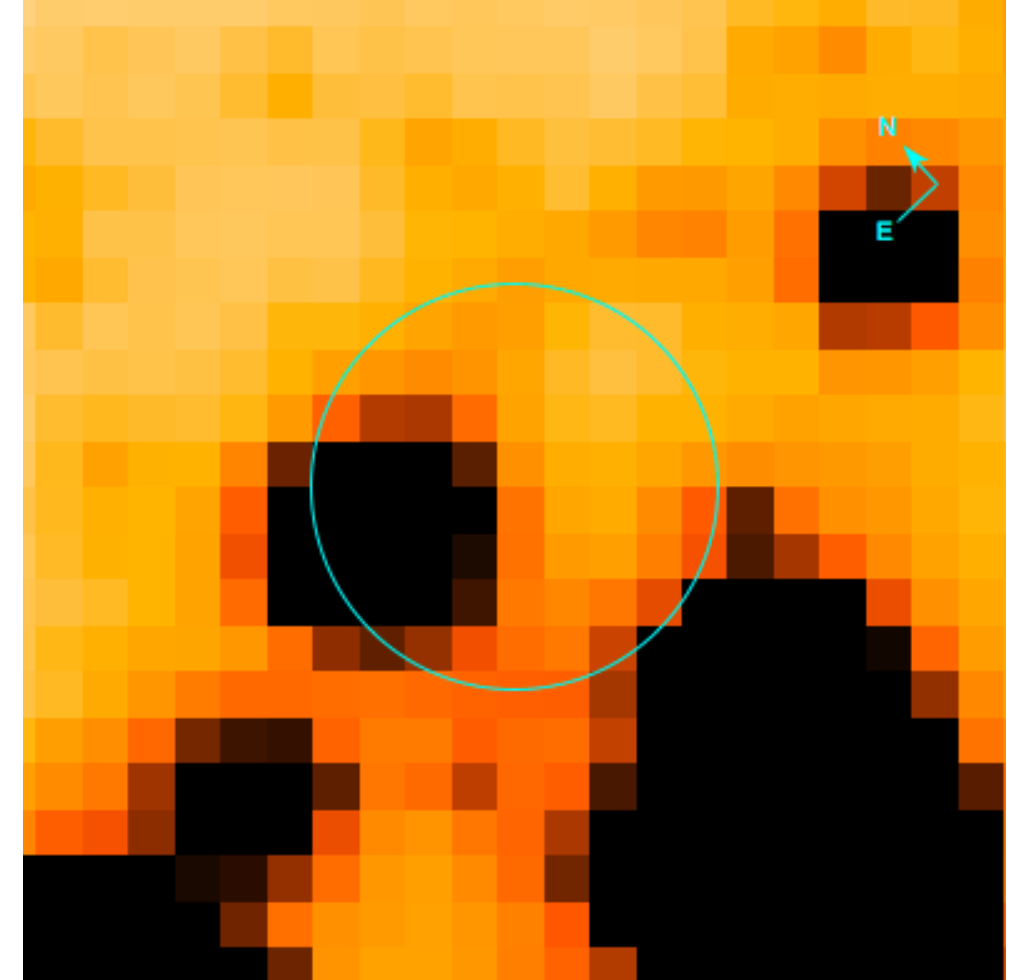
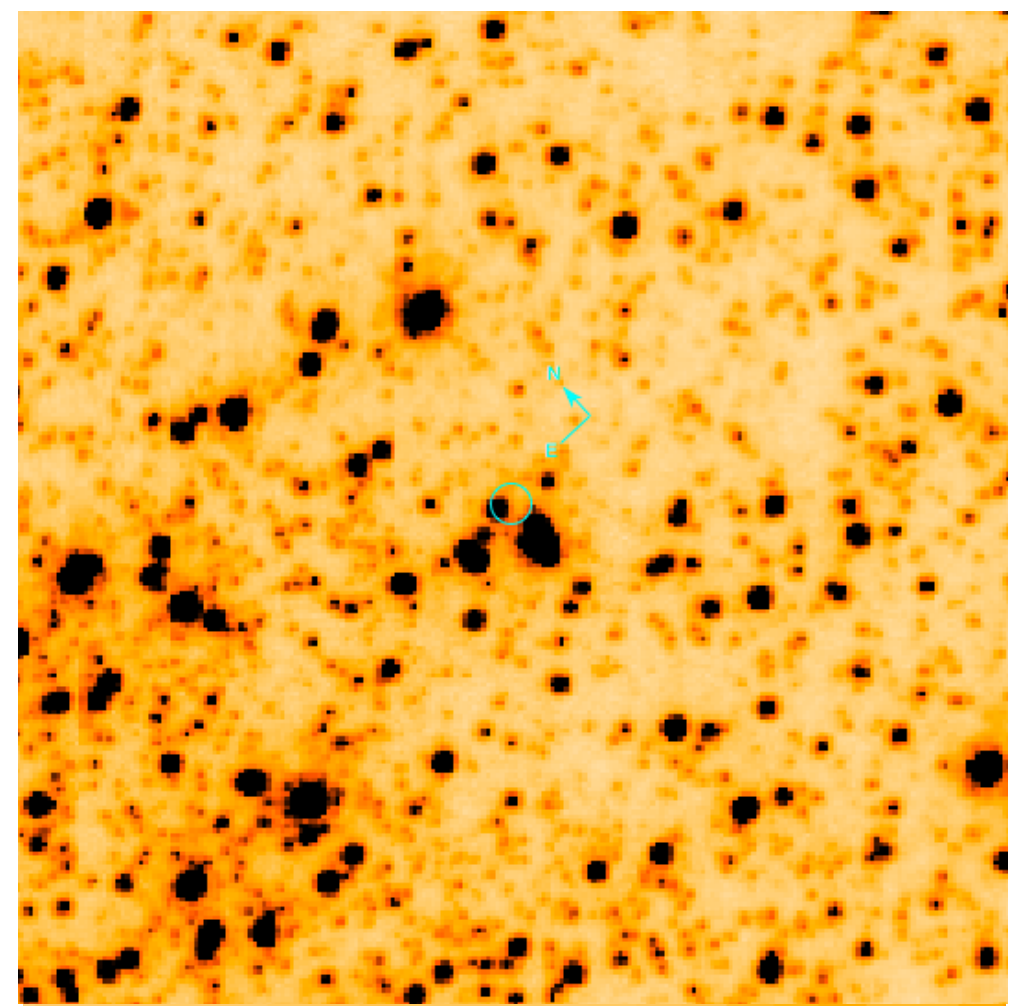
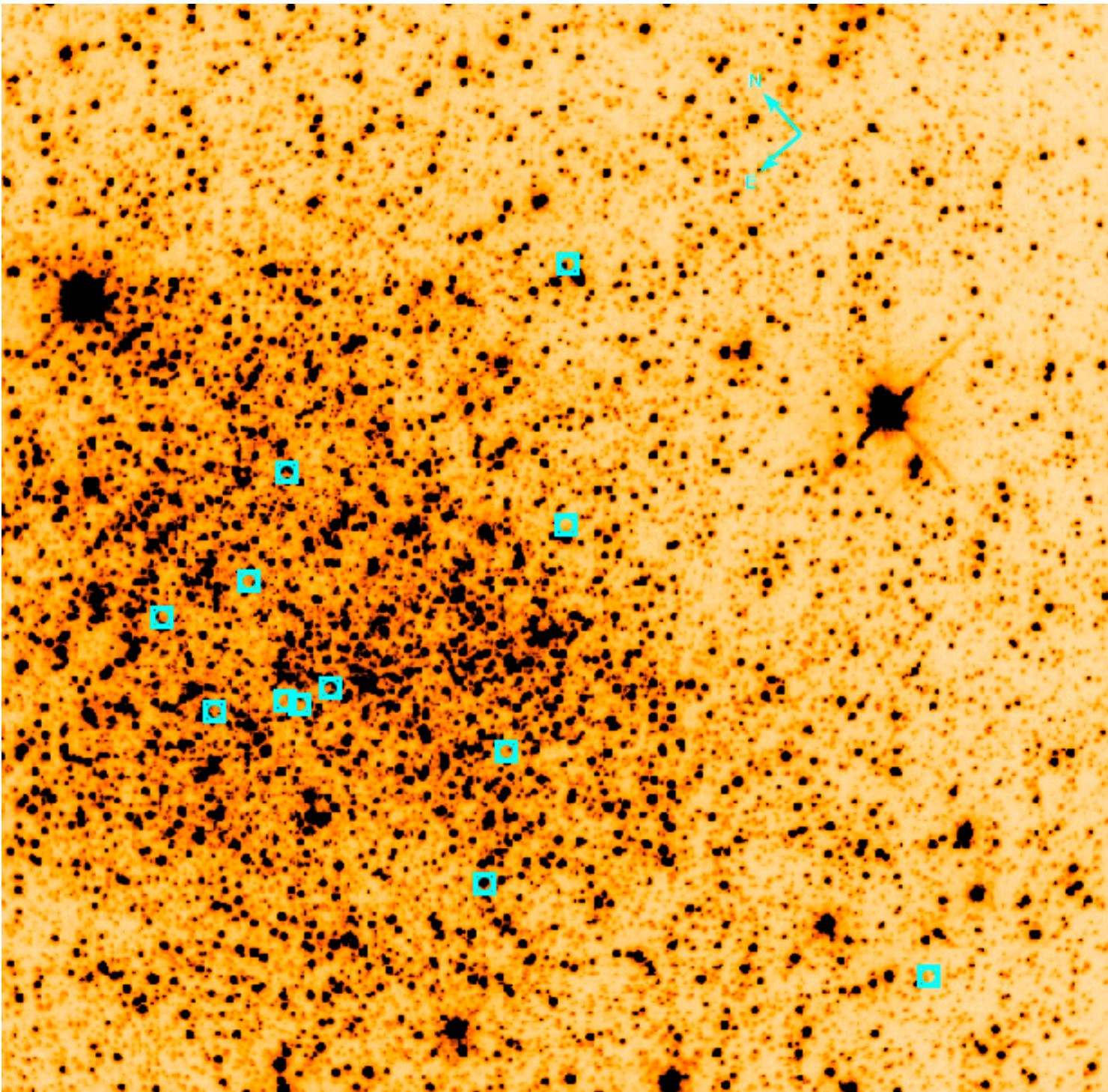
Black Widow and Redback pulsars

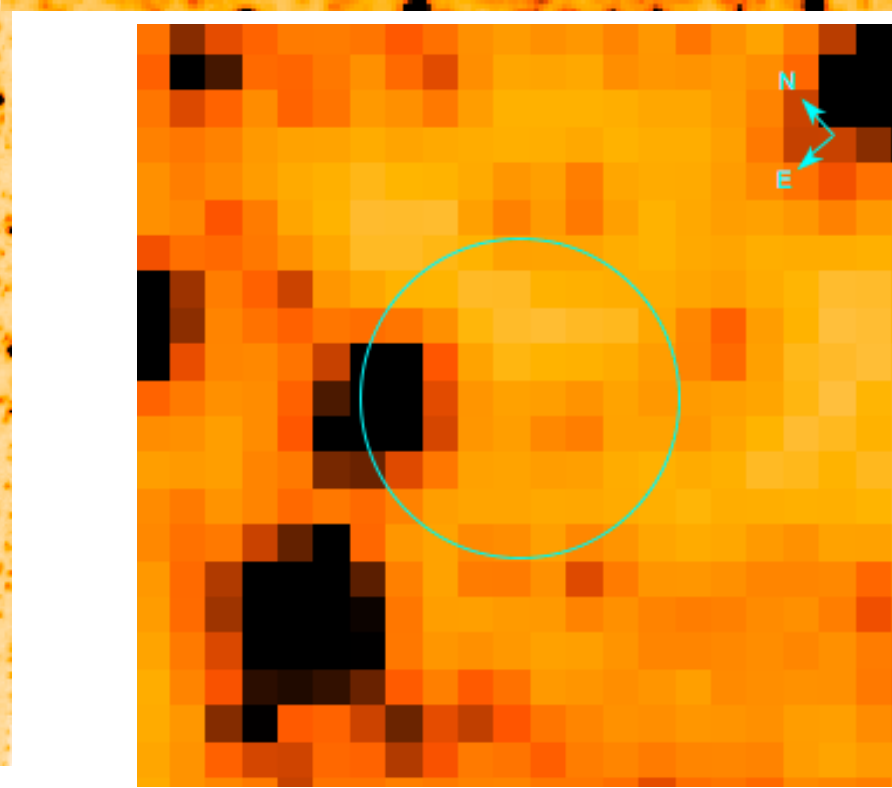
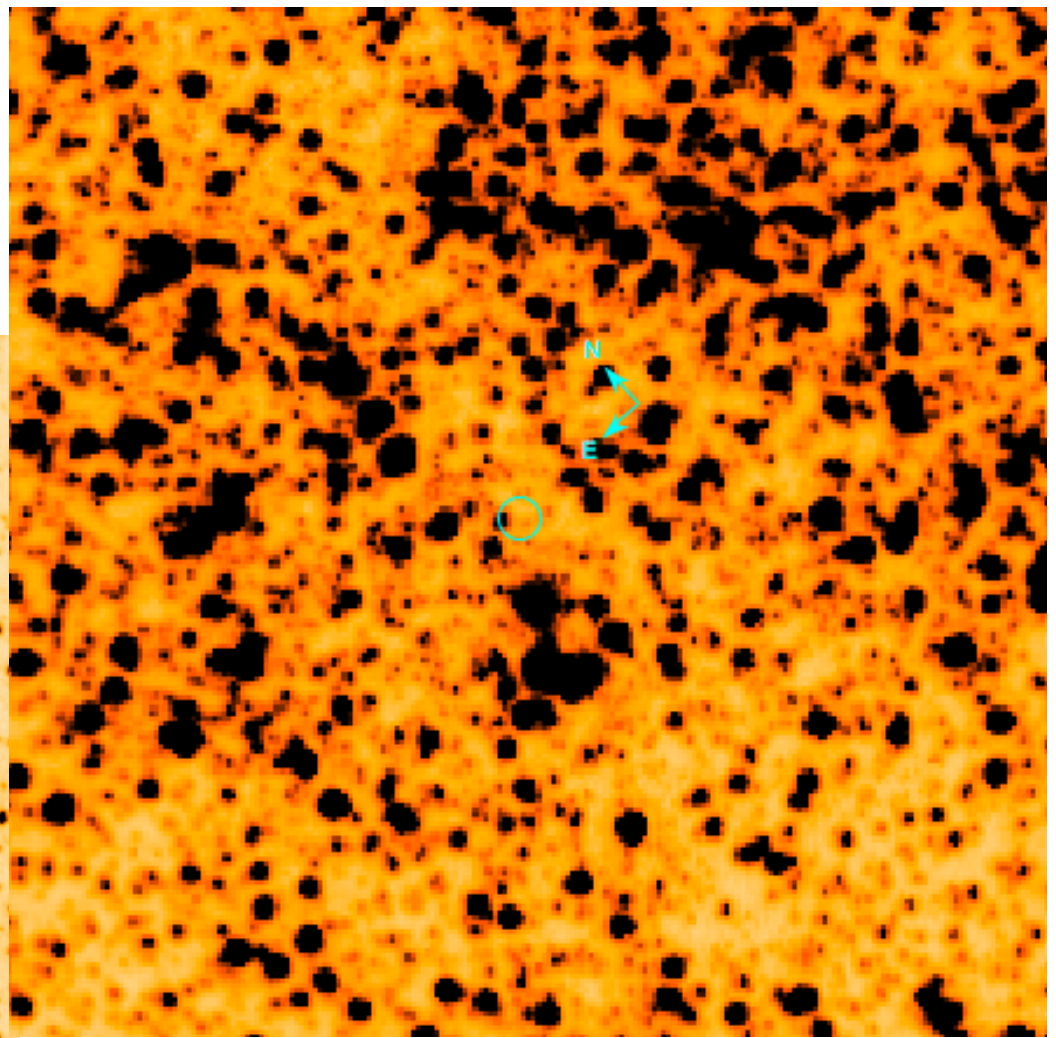
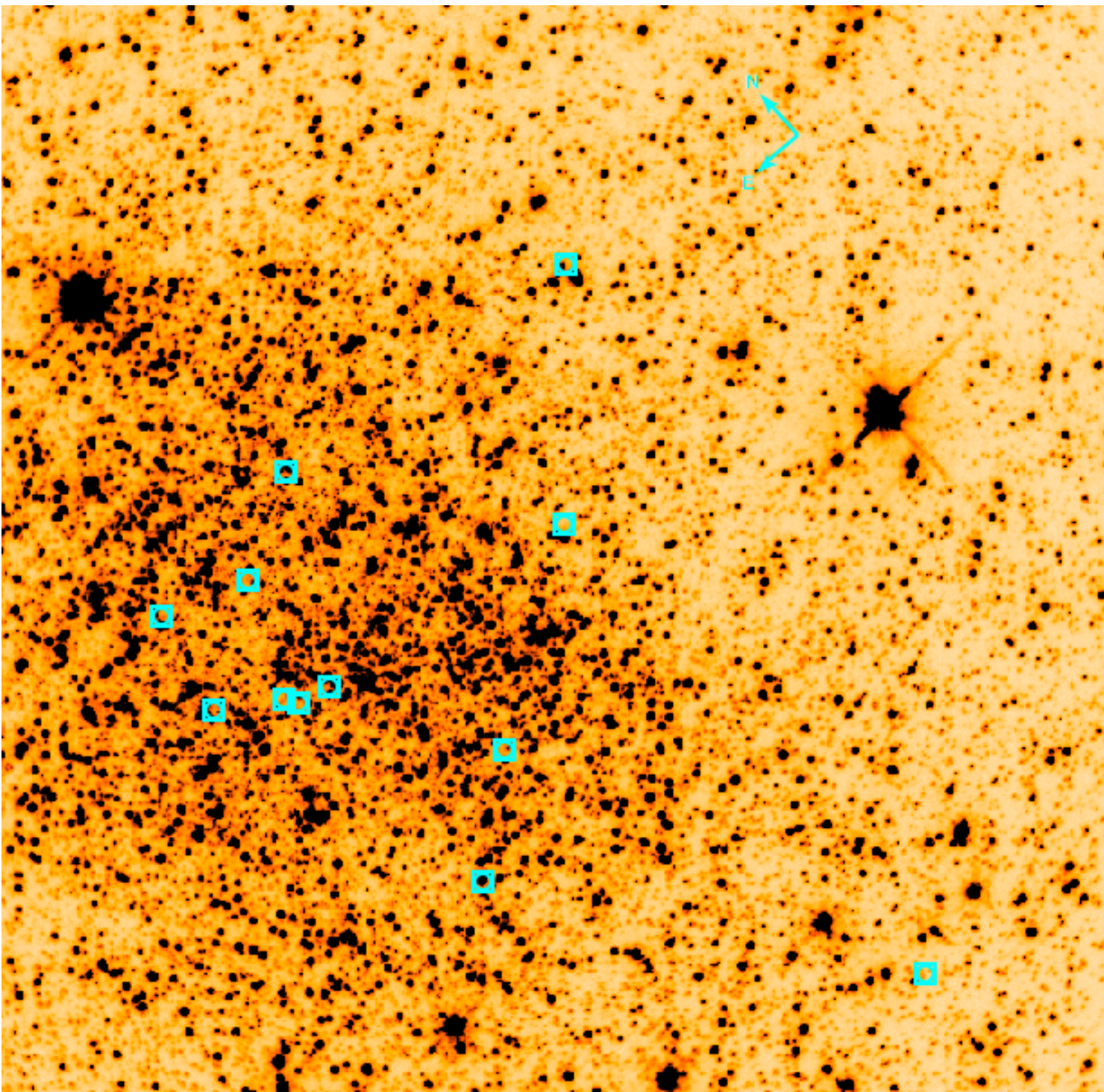
- Close binary orbits
- orbital periods from < 2 hours
- companion mass down to $0.01 M_{\odot}$, can be less
- comprehensive evolutionary path unclear : spectroscopy needed



Movie credit : NASA's Goddard Space Flight Center/Cruz deWilde

Terzan 5 : Archival :
F606W / WFPC2





HTRA Science Case II Close Binary Systems

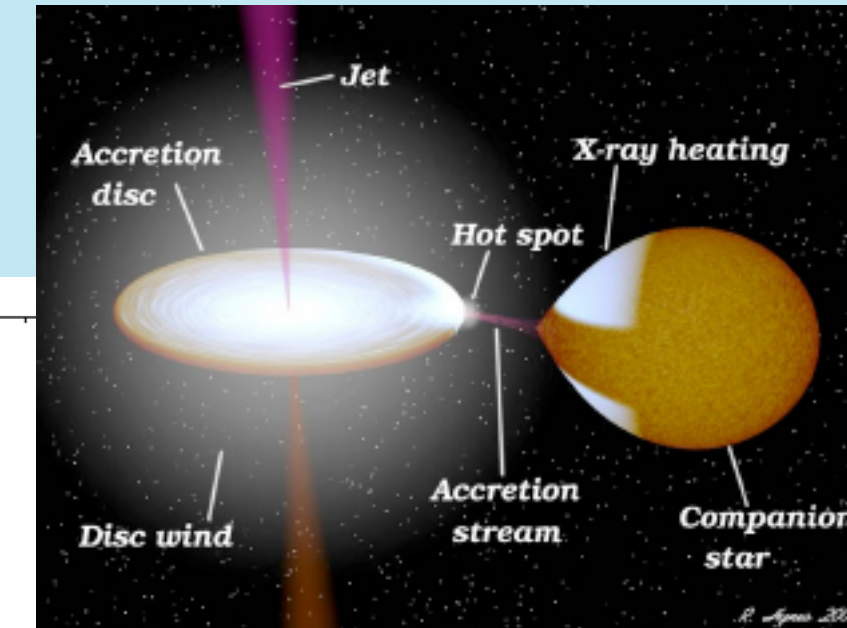
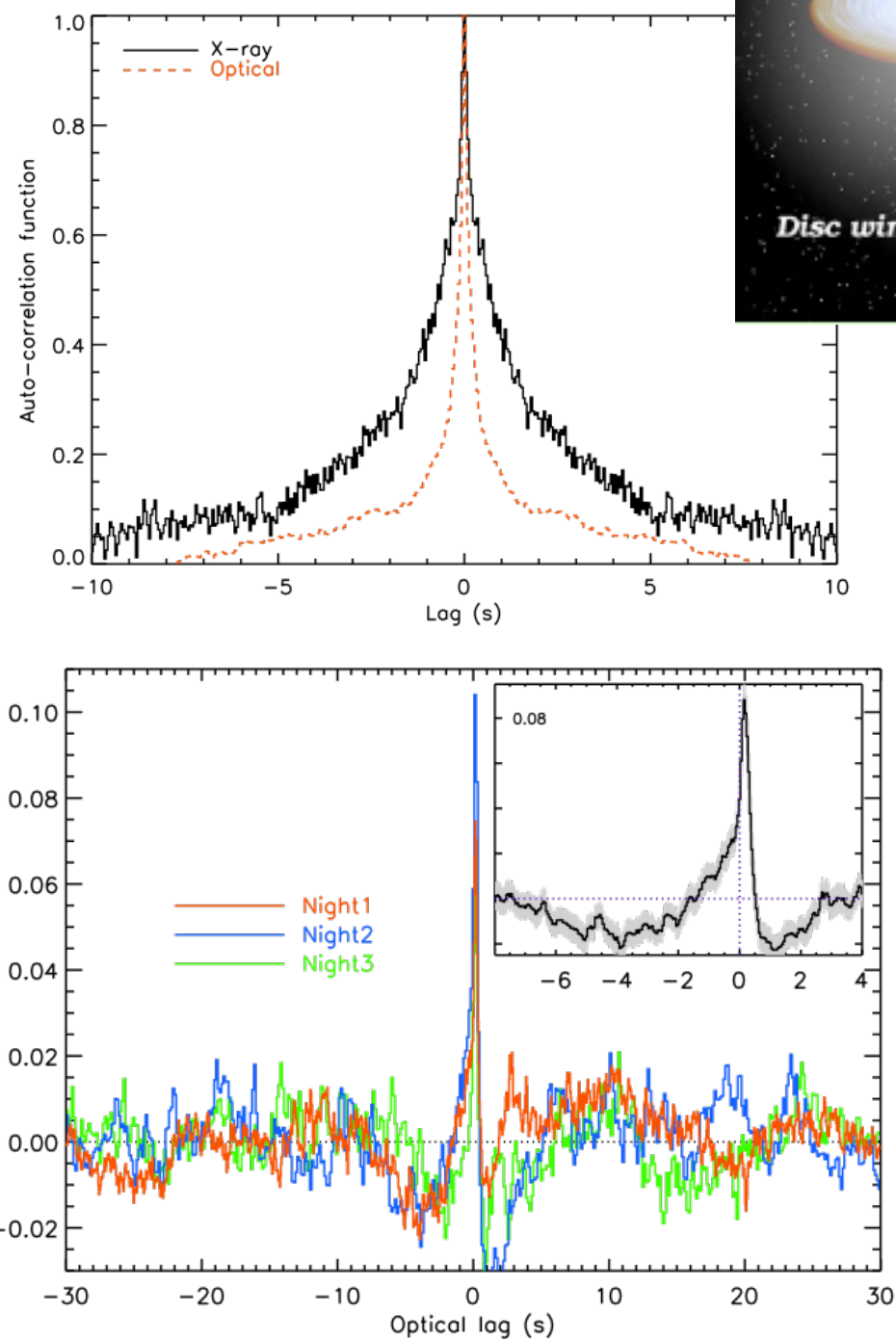
X-ray-Optical cross-correlations
observed by UltraCam and Optima

Shown are UltraCam observations of
the black-hole accretor GX339-4 -
Gandhi et al (2008)

Time scales < 1 sec

Optical Autocorrelation indicated
synchrotron emission from a possible
jet structure rather than being driven
by X-ray reprocessing.

GX339-4 is reasonably bright $V \sim 17$.
Other objects considerably fainter -
E-ELT required to look at spectral
variability



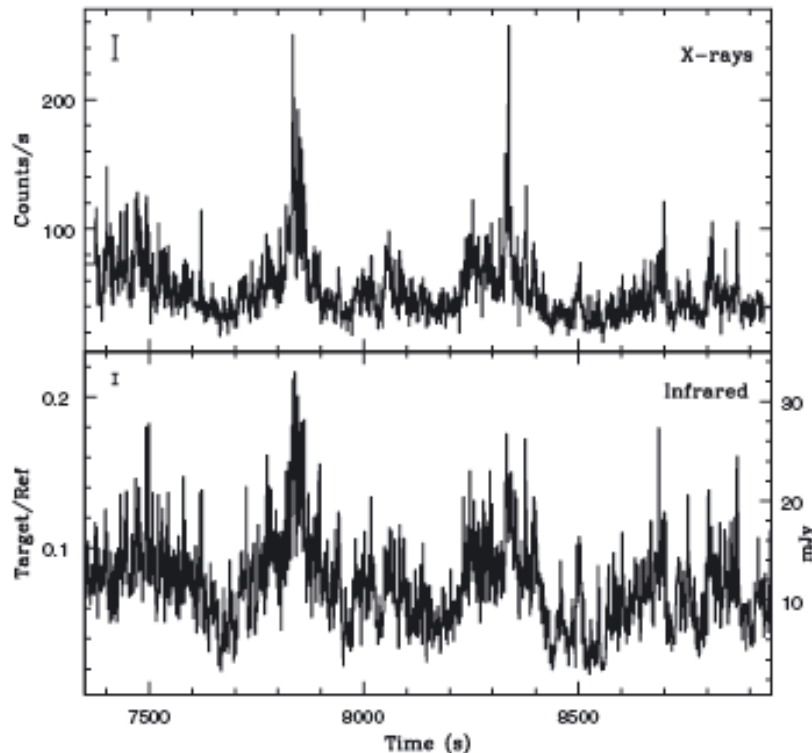


Figure 1. Top panel: a sample of the X-ray light curve of GX 339–4, obtained with the PCA onboard *RXTE*. The data are background subtracted, in the 2–15 keV energy range, at 1-s time resolution. Bottom panel: the simultaneous IR light curve, obtained with ISAAC. We show the ratio of the source (average 4.4×10^5 counts s^{-1}) to the reference-star (6×10^6 counts s^{-1}) count rates in the K_S filter, at 1-s time resolution. The right ordinates show the dereddened flux. We show the typical error bars in the top left-hand corner of each panel.

**Variable IR emission coming from jet near the BH, 100 ms delay wrt X-ray emission
Time resolved polarimetry is important**

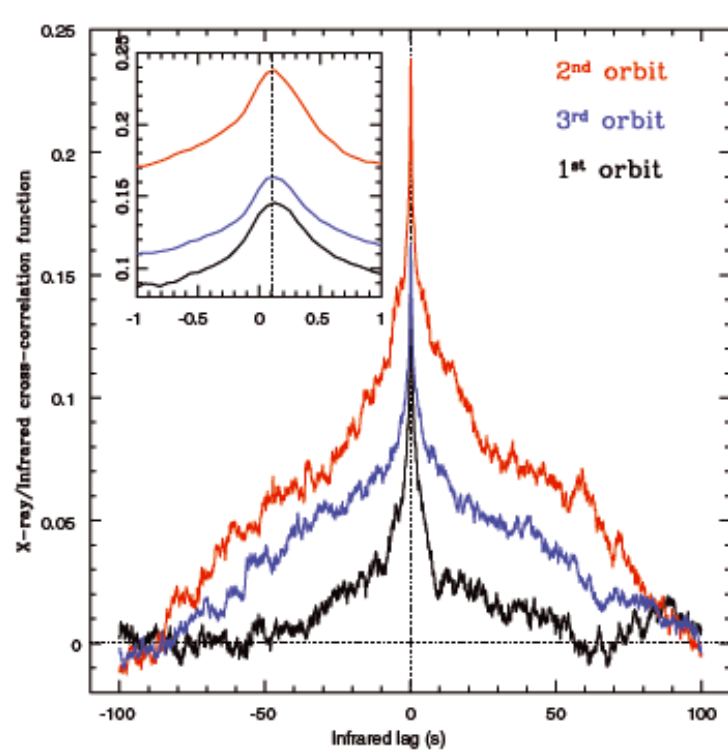


Figure 2. Cross-correlations of the X-ray and IR light curves of GX 339–4 (positive lags mean IR lags the X-rays). A strong, nearly symmetric correlation is evident in all the three time intervals, corresponding to different *RXTE* orbits. In the inset, we show a zoom of the peaks, showing the IR delay of ~ 100 ms with respect to the X-rays. The inset also shows a slight asymmetry towards positive delays.

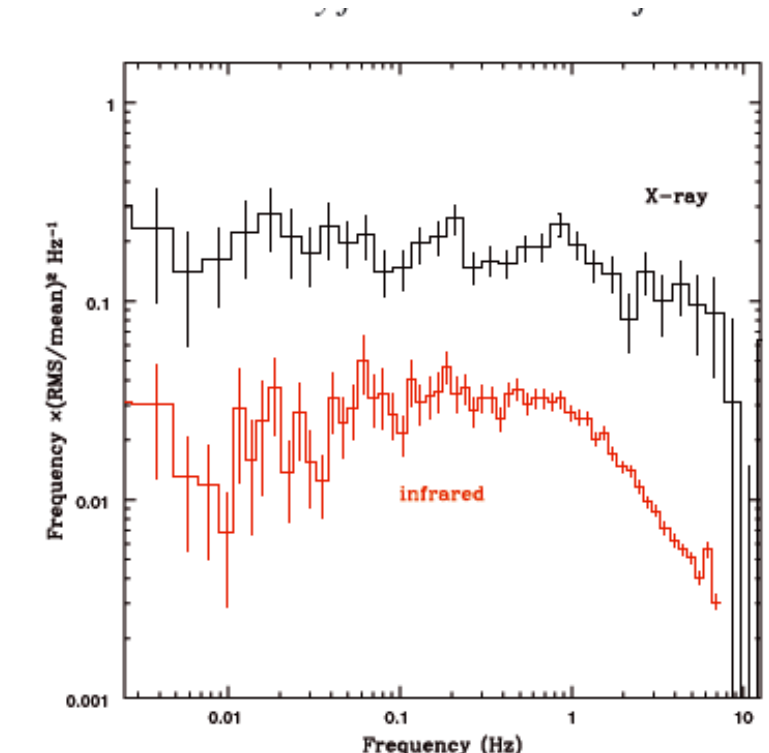


Figure 3. X-ray (2–15 keV) power spectrum of the second *RXTE* orbit (upper curve), together with the power spectrum of the simultaneous IR light curve (lower curve). The Poissonian noise has been subtracted from both the spectra. The peak at ~ 6 Hz in the IR spectrum is instrumental. The high-frequency portion of the IR spectrum has yet unmodelled systematics, which however do not affect the results presented here.



fundamental
radiation
physics

E-ELT 0.004 s-hours

Pulsars: giant pulses,
lightcurves & polarisation

Black hole systems: jets,
accretion & transients

Existing
instruments
 \sim ns - ms

Neutron star systems:
'magnetars', accretion &
transients

WD binaries:
accretion

ns

μ s

ms

s

hr

characteristic timescale

fundamental
radiation
physics

Pulsars: giant pulses,
lightcurves & polarisation

Black hole systems: jets,
accretion & transients

Neutron star systems:
'magnetars', accretion &
transients

WD binary
accretion

E-ELT 0.004s-hours

APDs

MKIDs

EMCCDs

frame transfer

ns

μs

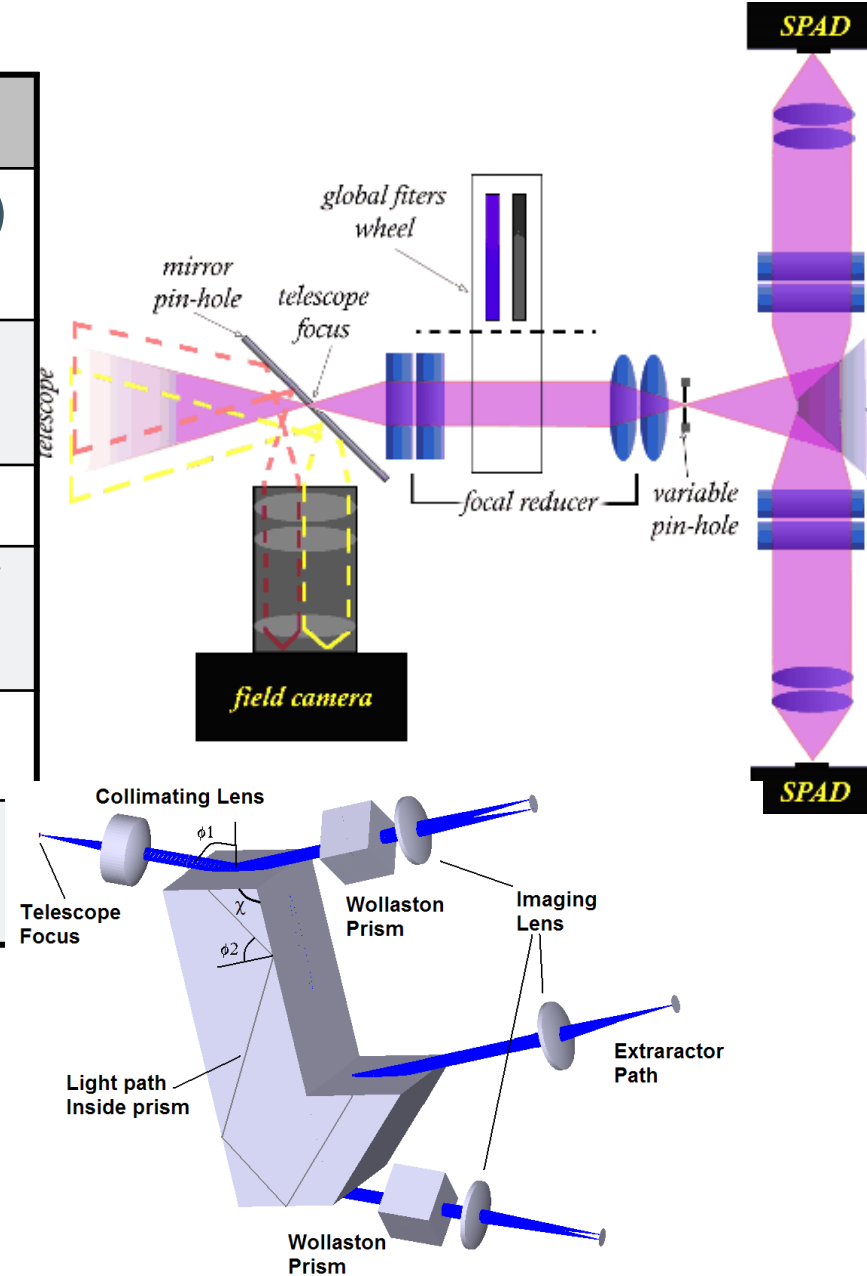
ms

s

hr

characteristic timescale

Instrument	Detector	Group	τ (ms)	Type
UltraCam	Frame Transfer	Sheffield/ Warwick	5ms	Imager (3-Band)
UltraSpec	EMCCD	Sheffield/ Warwick	1ms	Spectrograph
GASP	EMCCD	Galway	600 μ s	Polarimeter
Optima	APD	MPE	1 ns	Photoncounter / polarimeter
Iqueye	APD	Padua	0.1 ns	Photon counter
Arcons	MKID	UCSB	20 ns	Imager



ESO - HTRA : Richichi et al 2009

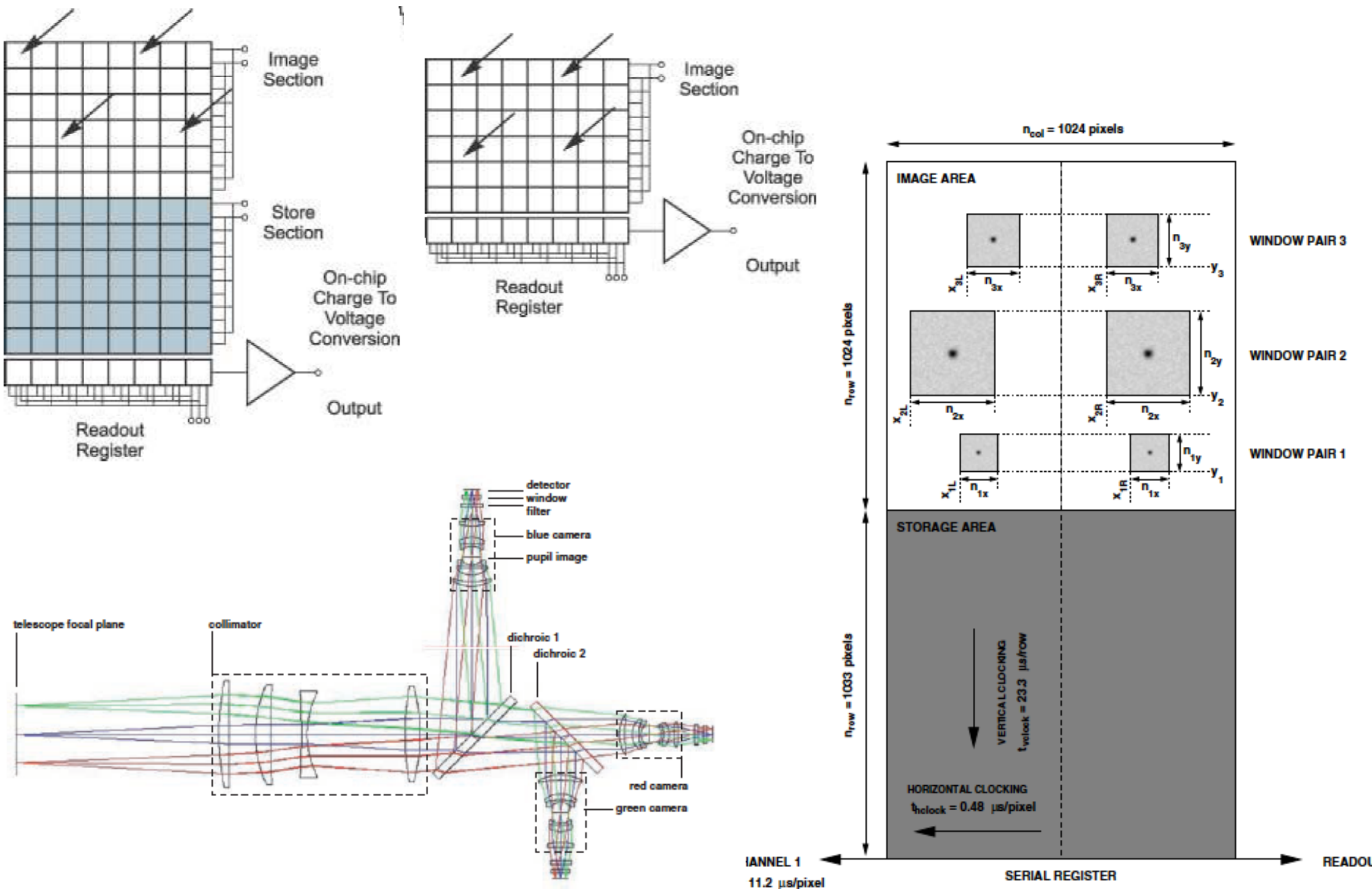
Instrument	Modes	Detector	Time Rate (Window)
VISIR	Burst	DRS	12.5 ms SF
SOFI	Burst, FastPhot	Hawaii	4 ms (8 x 8), 15 ms (32 x 32)
ISAAC	Burst, FastPhot	Hawaii-1, Aladdin	3 ms (32 x 32), 6 ms (64 x 64)
ISAAC	Burst	Hawaii-1, Aladdin	9 ms (1024 x 16)
NACO	Cube	Aladdin	7.2 ms (64 x 64), 350 ms (1024 x 1024)
HAWK-I	Fast	Hawaii-2RG	6.3 ms (16 x 16)
FORS2	HIT	CCD (charge shift)	up to 2.3 ms
VLTI	Fast	Various	up to 1 ms

Taken from Kieran O'Brien's talk at Galway workshop

	sensitivity	Noise	Time resolution	Energy resolution	Array size	Cost/unit
• Eyes	Poor	Good	msec	Poor	Good	Free
• Photographic plates	Fair	Poor	minutes	none	Good	Moderate
• Photomultipliers	Fair	Good	< μ sec	none	Poor	High
• CCDs	Excellent	Good	seconds	none	Excellent	Moderate
• CMOS	Excellent	Fair	seconds	none	Excellent	Moderate
• APD	Fair	Good	< μ sec	none	Poor	High
• STJ	Fair	Excellent	μ sec	Fair	Poor	High
• TES	Fair	Excellent	μ sec	Fair	Poor	High
• MKIDs (2020)	Excellent	Excellent	μ sec	Fair	Good	Moderate

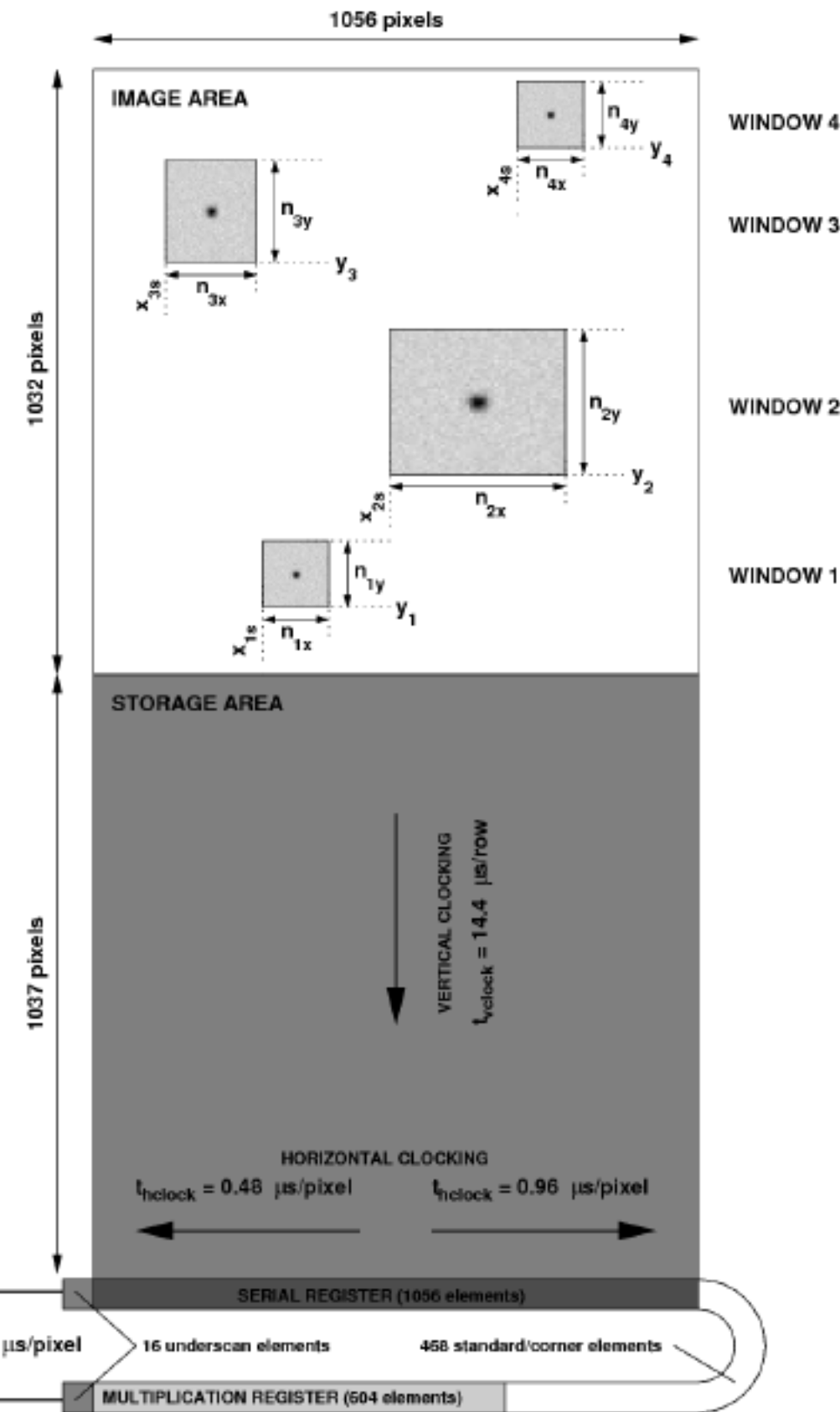
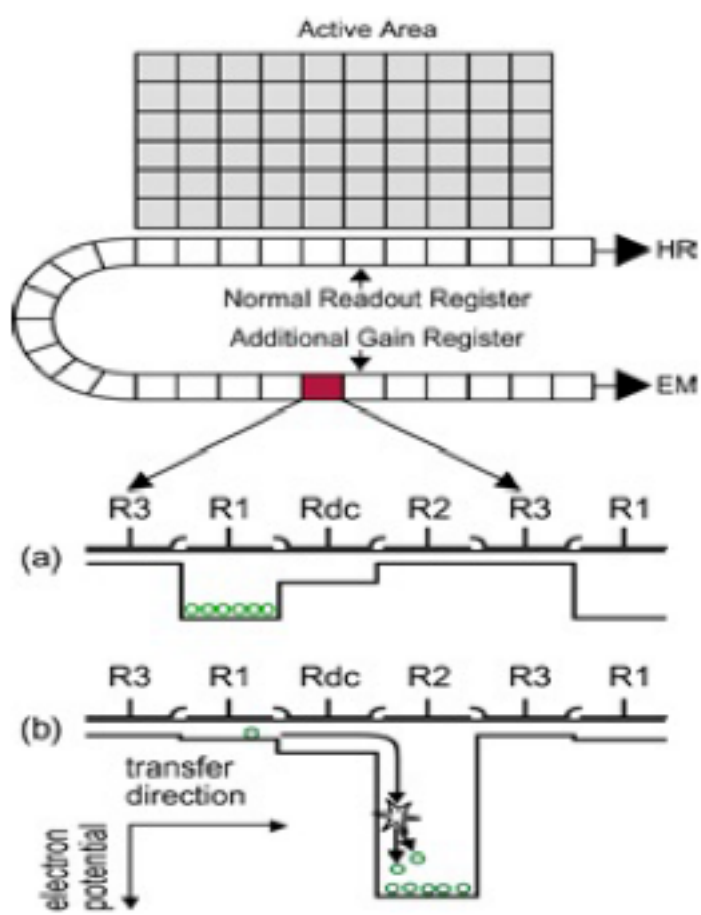
- Frame Transfer : UltraCam, $t_{\min} \sim 4$ ms

Dhillon et al, 2007, MNRAS, 378, 825



- Electron Multiplying CCD, EMCCD or L3CCD :
UltraSpec, GASP, LuckyCam, $t_{min} \sim 600 \mu s$

- Reduced noise by amplification during readout
- see e.g. Basden et al, 2003,
MNRAS, 345, 985
- Subject to amplification noise
and stability problems

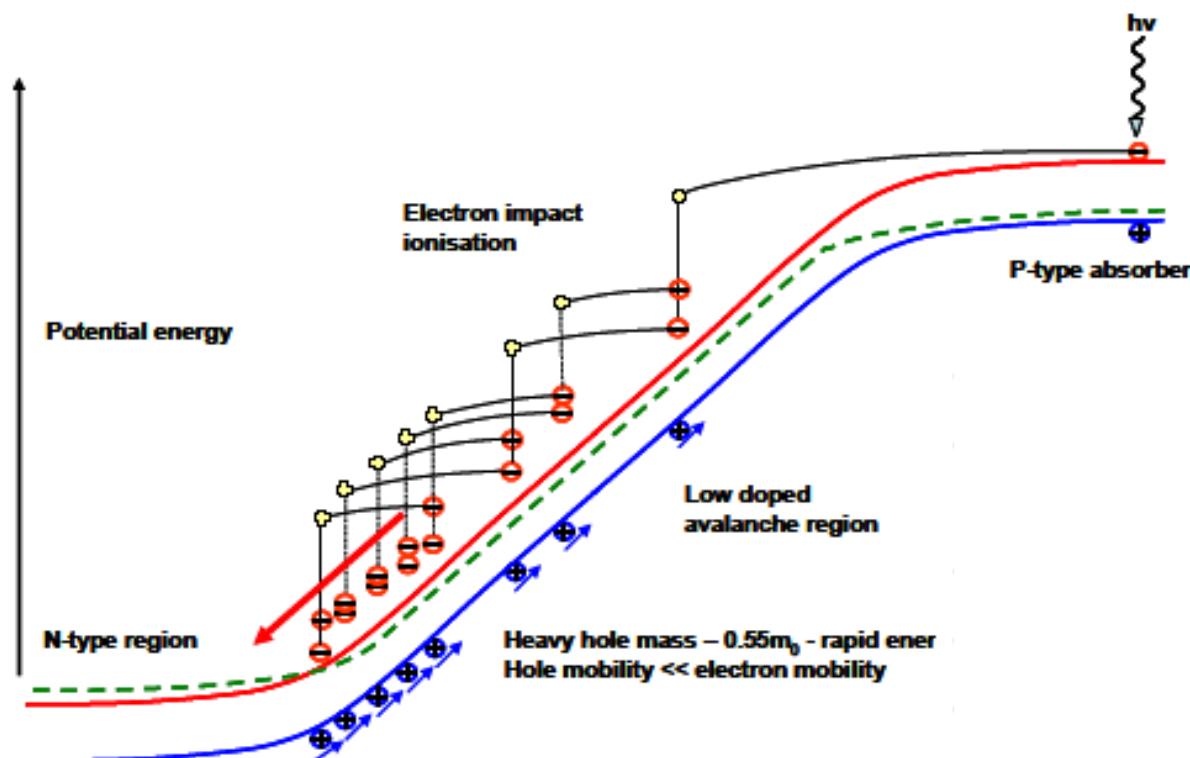


Avalanche Photodiode (APD), Optima, Iqueye single pixel, $t_{min} \sim ns$, or arrays - eAPDs

Optima : Straubmeier et al, 2001, Exp. Ast, 11, 15

Iqueye : Naletto et al, 2009, A&A, 508, 531

APD arrays : Finger et al, 2014, SPIE, 9148, 17



Fast - potentially low noise set by dark current
SAPHIRA detector initially for wave-front sense - sub-electron read noise

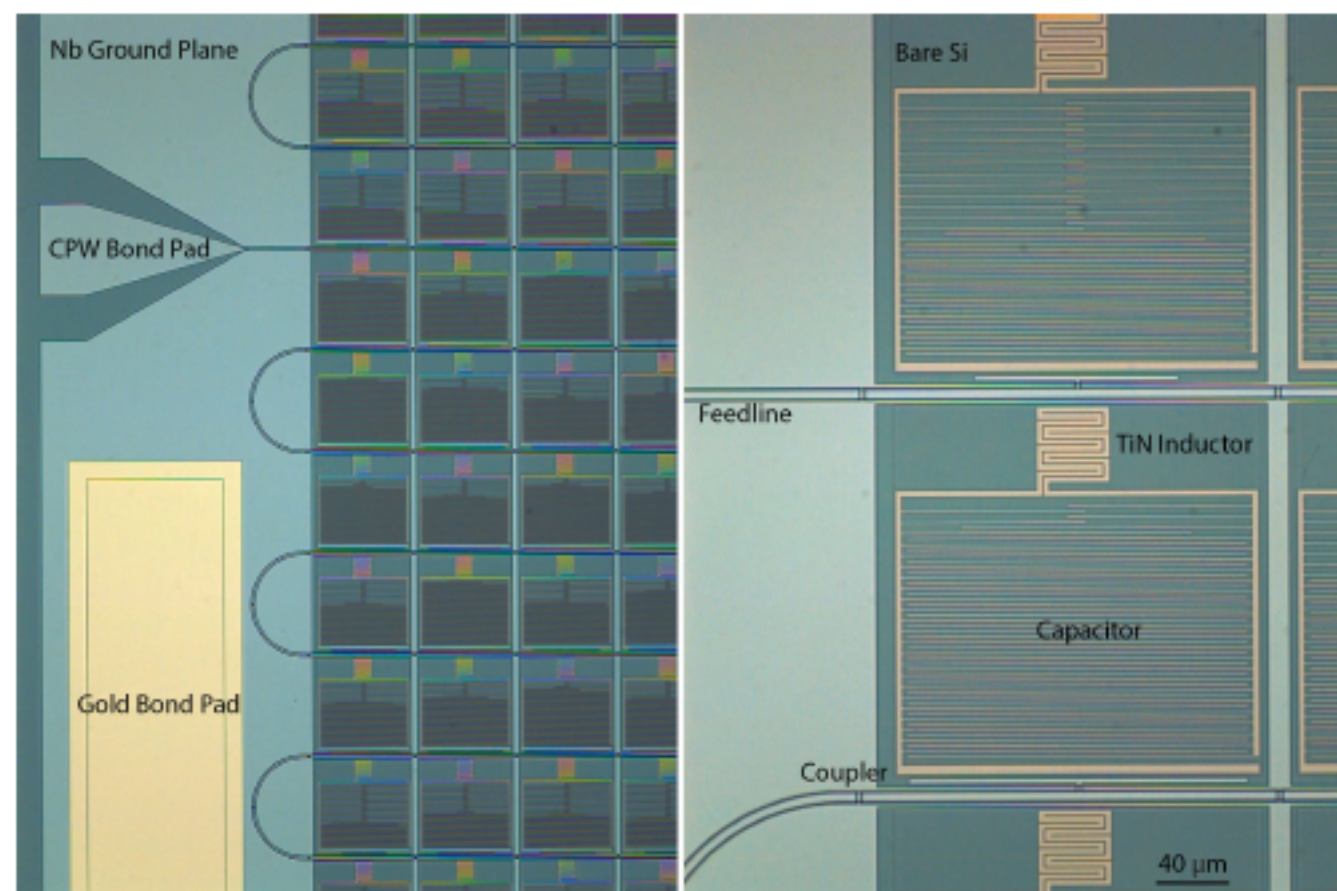
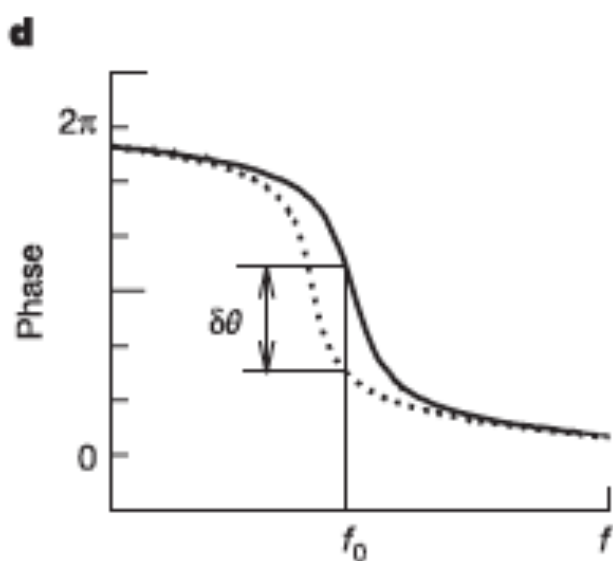
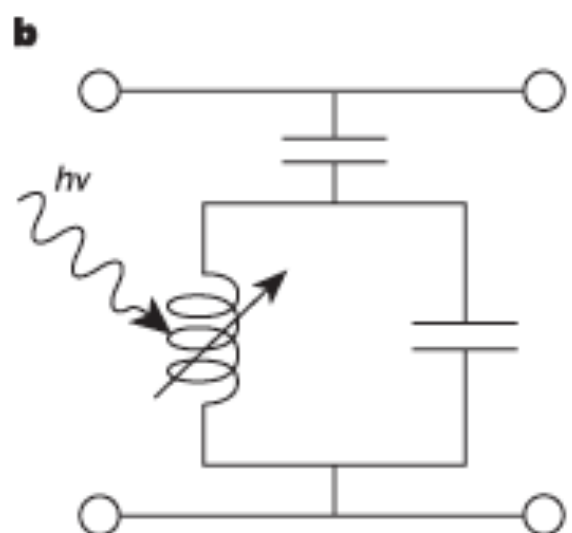
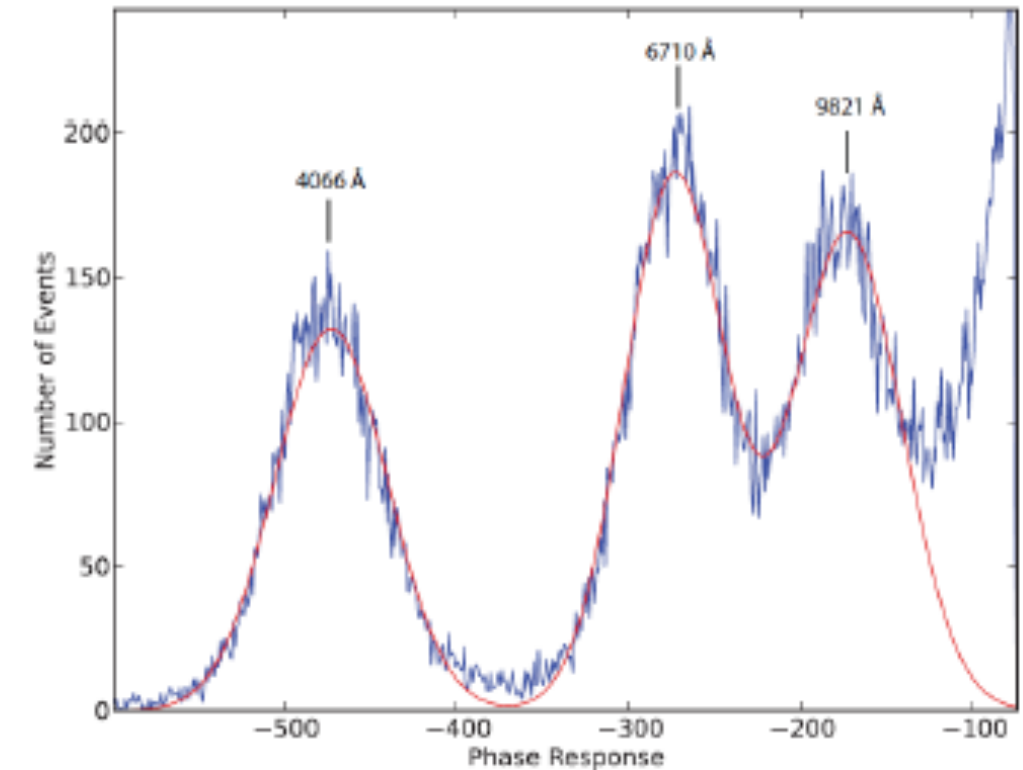
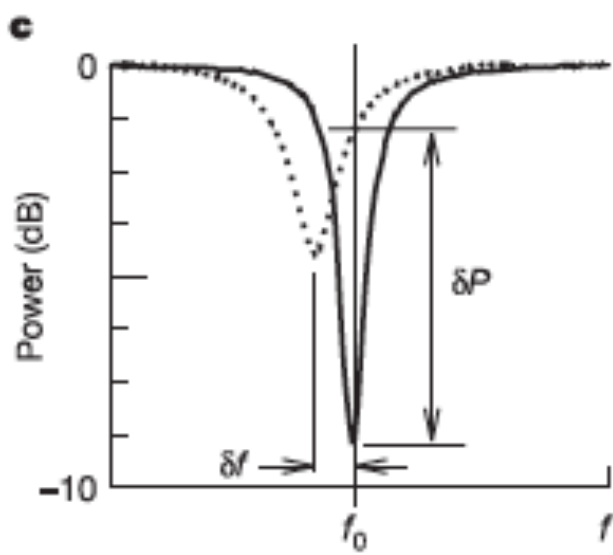
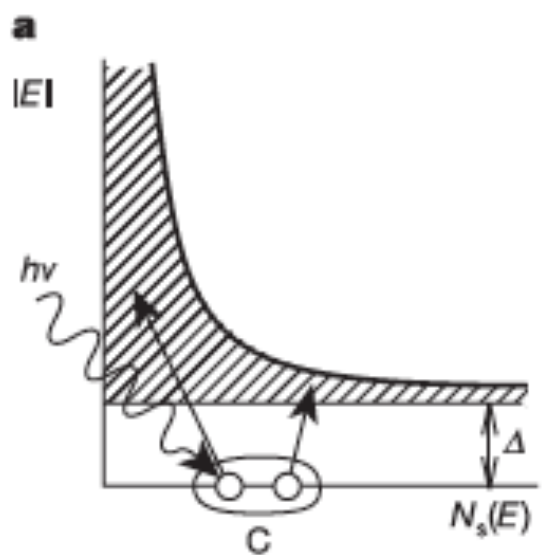


NUI Galway
OÉ Gaillimh



Microwave Kinetic Induction Detectors MKIDs, $t_{\min} \sim$ few ns

ARCONS : Mazin et al, 2013, PASP, 125, 1348

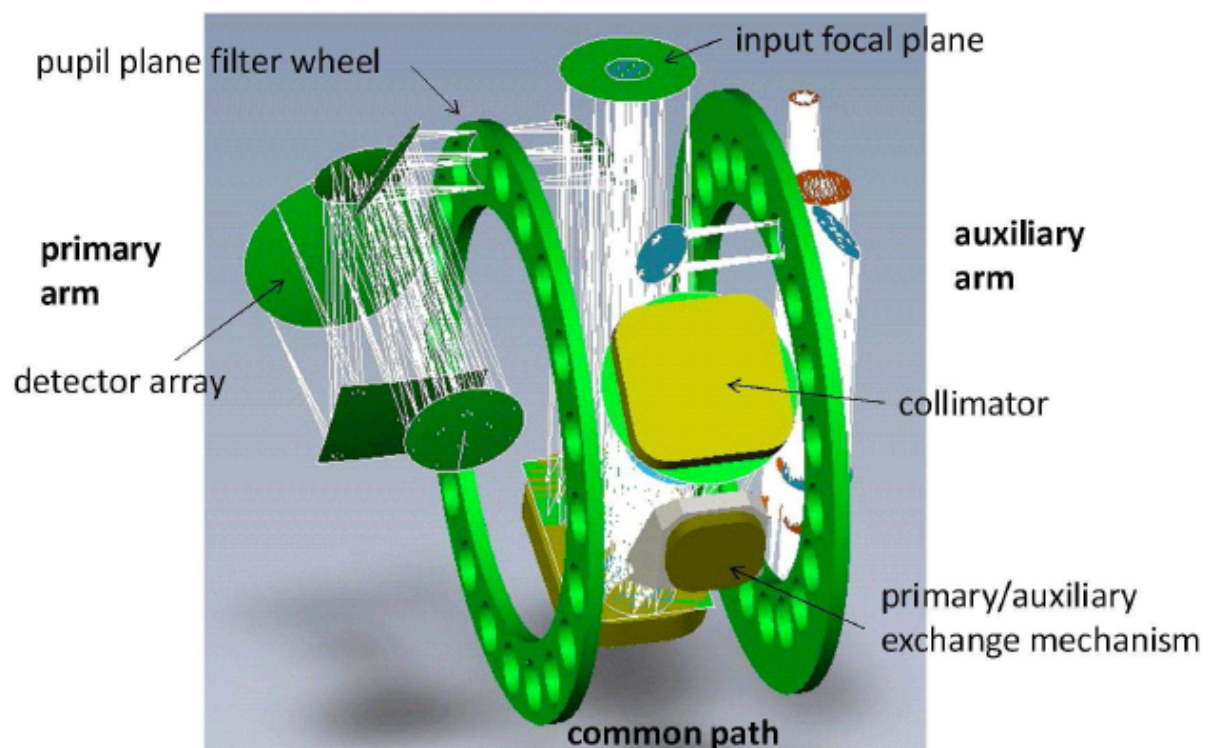


NUI Galway
OÉ Gaillimh

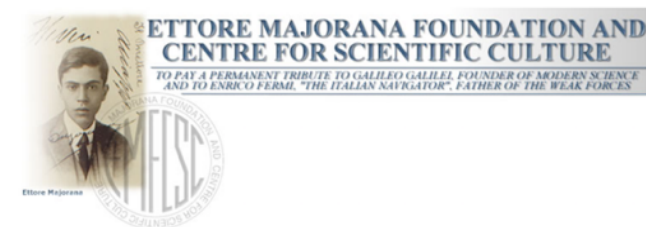


Micado : HTRA Contribution

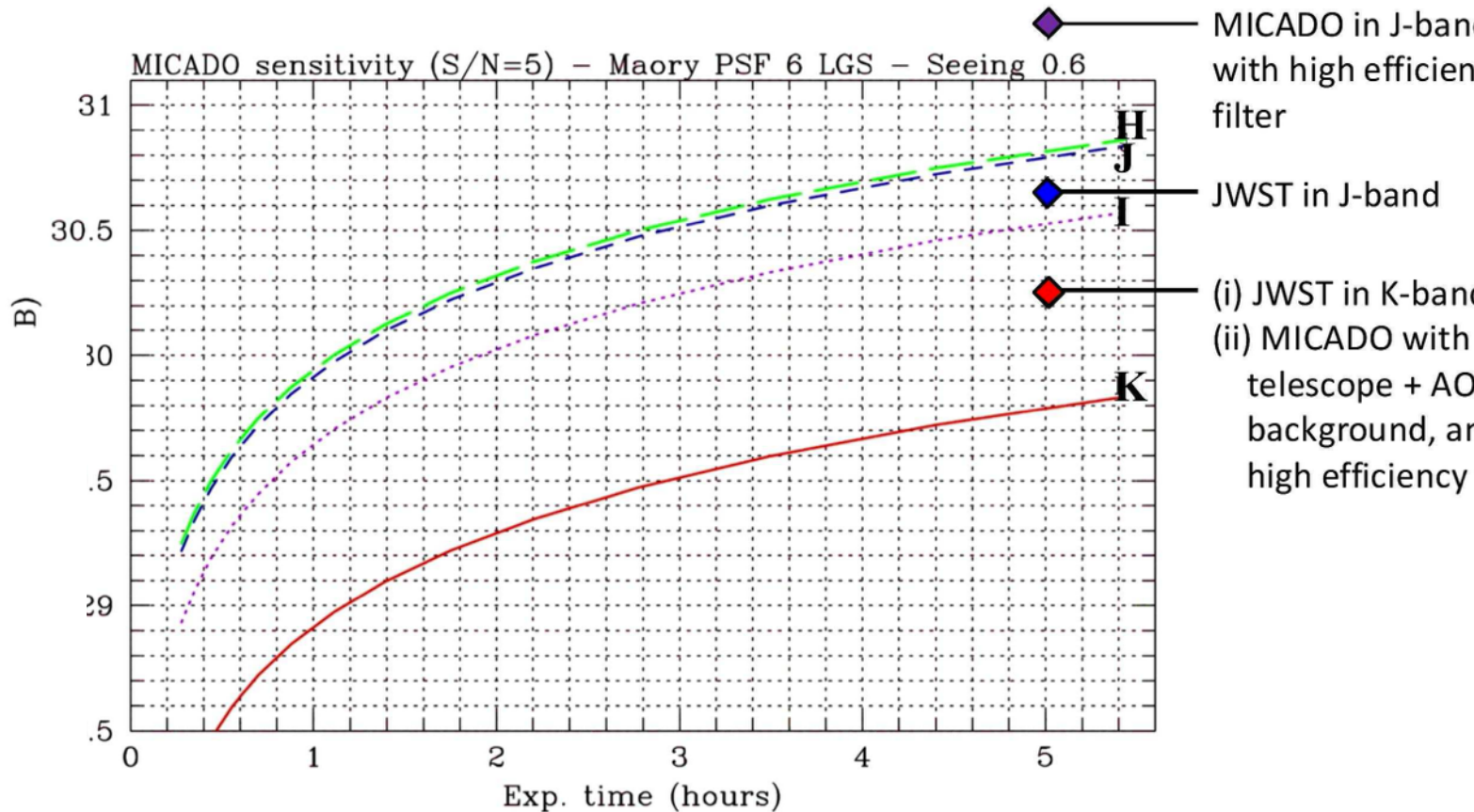
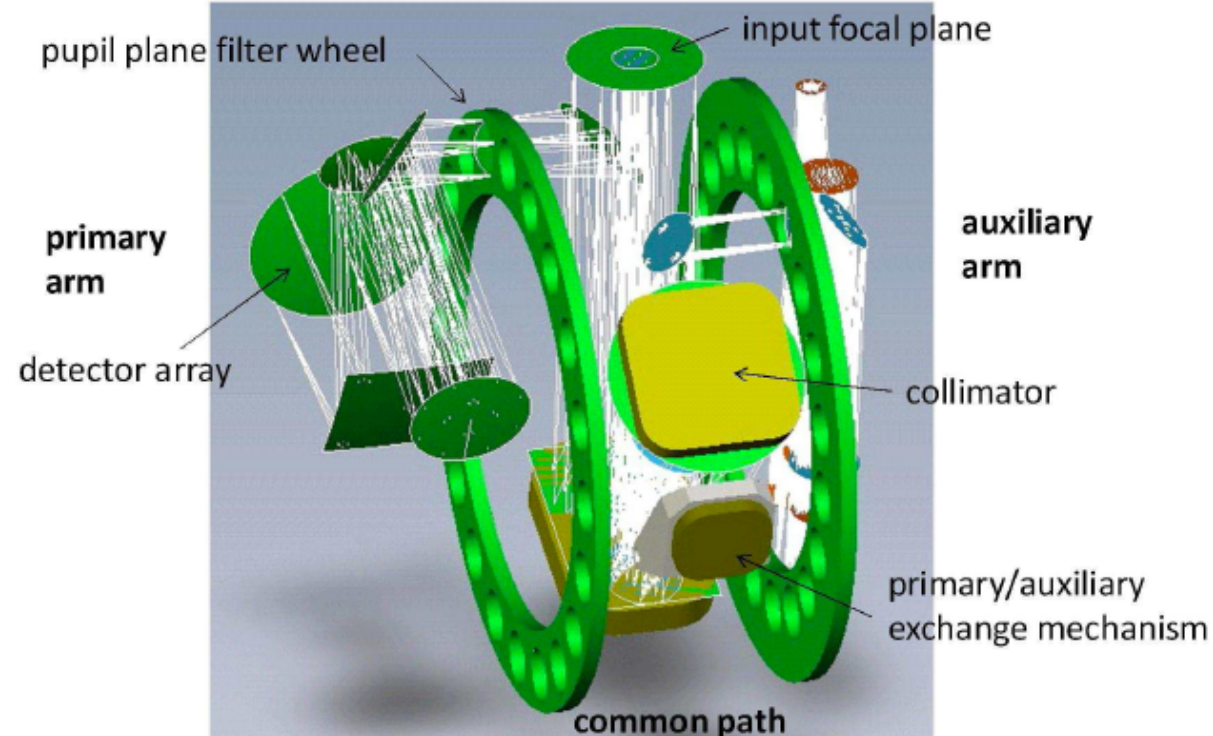
- High Sensitivity
 - optical pulsar detection down to $m_k \sim 30$ [maybe hundreds]
- Timing
 - magnetar light curves down to $m_k \sim 25$ [10s]
 - some pulsar timing
 - correlated observations - needs absolute timing
- Excellent Astrometry
 - pulsar proper motion
- No polarimetry



NUI Galway
OÉ Gaillimh



Micado



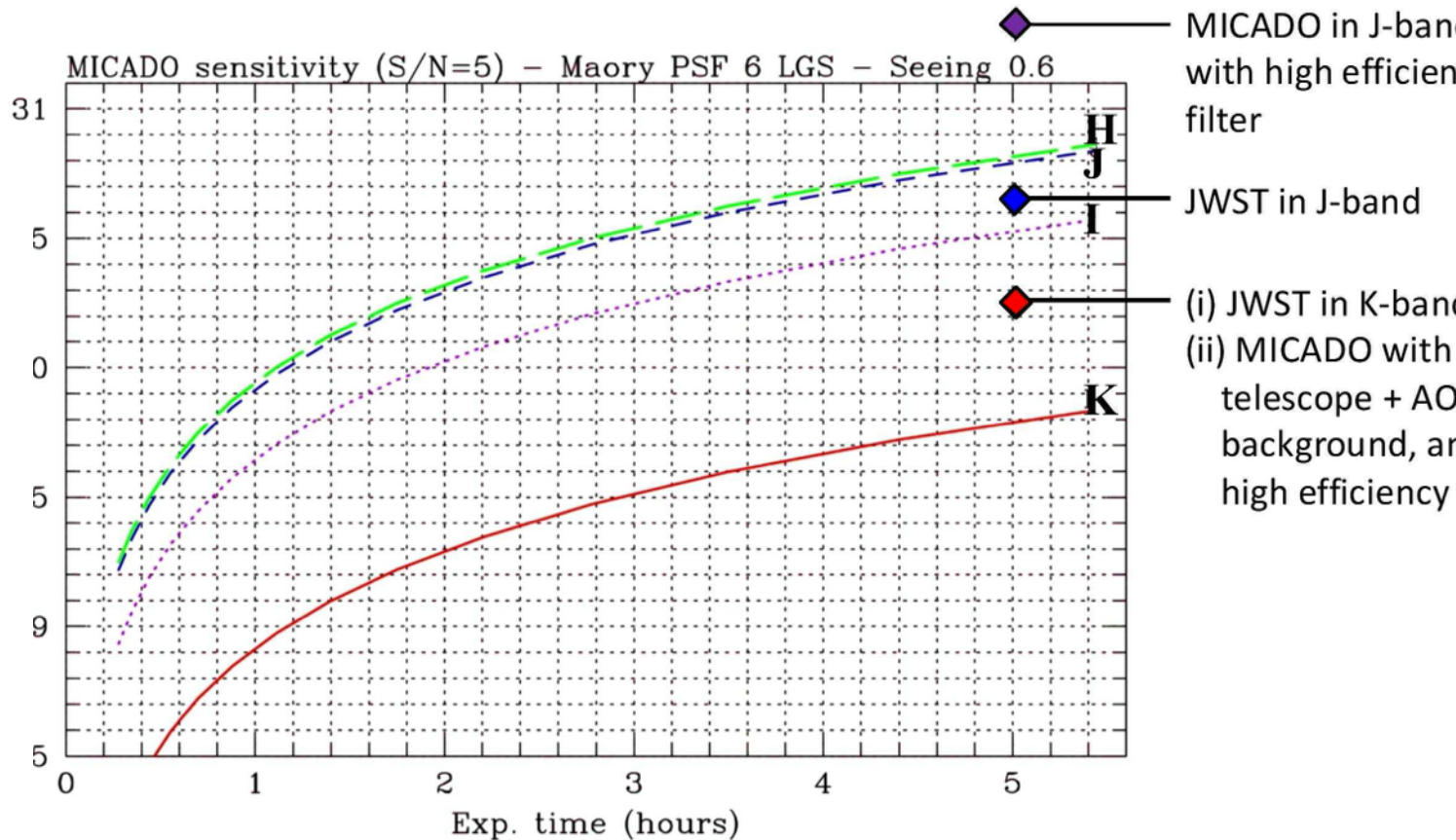
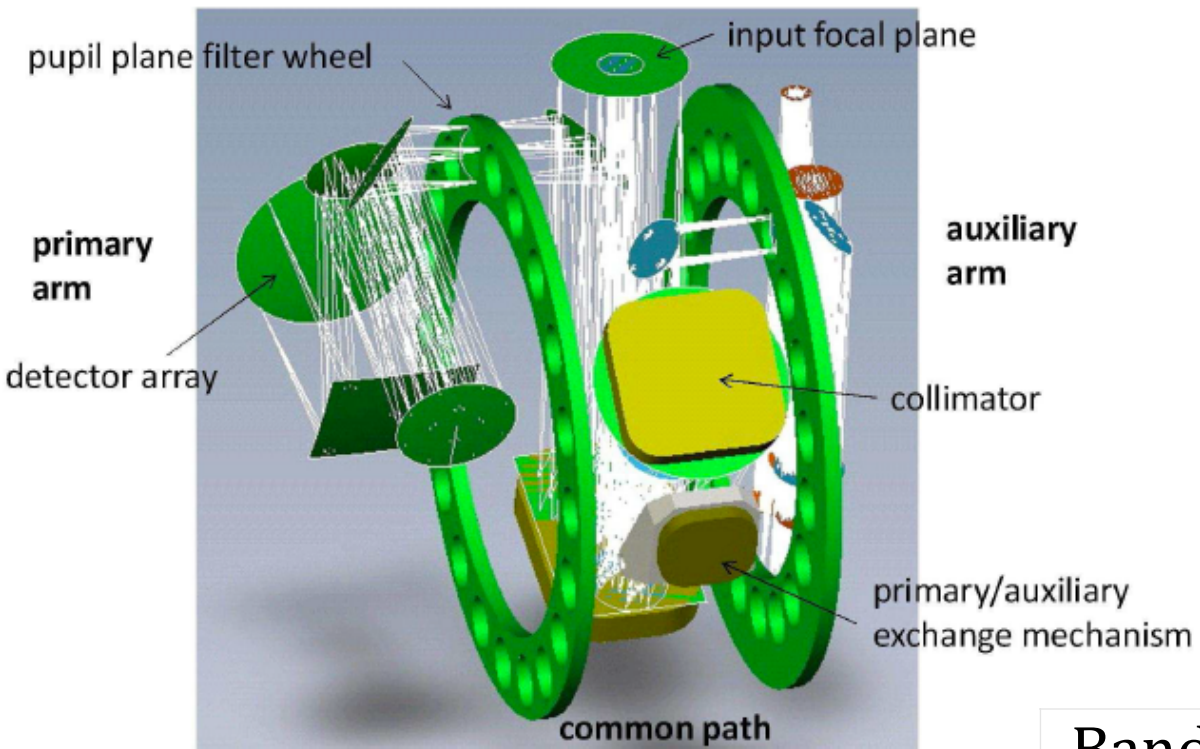
All 2.5 Hz **Read Noise** **e⁻ / frame**
e⁻ / frame **m_{JHK}=23.5**

J 2x2	8.5	10
--------------	------------	-----------

H 2x2	10.7	23.3
--------------	-------------	-------------

K 4x4	22.5	25
--------------	-------------	-----------

Micado

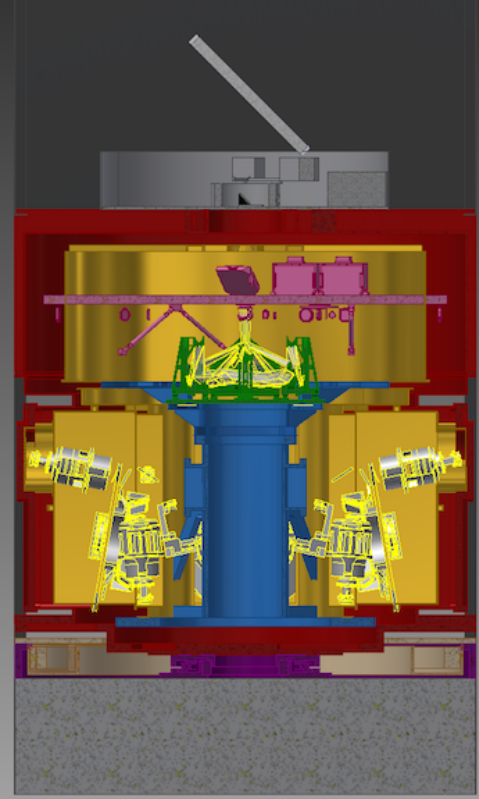


1σ Limiting
Magnitudes / frame:

Band	0.25Hz	2.5Hz	25Hz	250Hz
I (Z)	26.5	24.1	21.7	18.0
J	26.8	24.9	22.4	18.9
H	26.2	24.6	22.1	18.9
K	25.3	23.9	21.9	18.3

Harmoni :

- Spectroscopy of MSP secondaries in GC
- Magnetar/pulsar spectra down to $m \sim 25$
- But a frame transfer readout would give some time resolution



Thatte et al, 2014, Proc. SPIE, 9147, 25

Spectral	4 mas		10 mas		20 mas		30x60 mas	
Resolution	R _{AB}	H _{AB}						
Point source (AB mag)								
500		27.42		27.36		26.90		26.02
3500	22.93	26.64	23.89	27.44	24.69	27.53	25.64	26.98
7500		25.82		26.66		26.84		26.43
20000		24.76		25.63		25.87		25.63

Figure 4: Expected point source limiting magnitudes for HARMONI to achieve an SNR of 5 in 5 hours of on-source exposure time, under the conditions outlined above, for different spaxel scales and different spectral resolving powers.

- Summary
 - Timing from Micado
 - noise limited
 - JHK observations of magnetars up to $m_k \sim 25$
 - integrated observations of pulsars down to $\sim 28/29$
 - time tagging with GPS?
 - Harmoni - frame transfer?
 - Simultaneous or follow on observations
 - Polarisation / XIPE
 - SKA : pulsar population - MSP-Binary-GC spectroscopic and astrometric observations
 - Polarisation important for compact objects with high magnetic fields

A 3D rendering of a large telescope on the surface of Mars. The telescope has a large blue and white segmented dome. The interior of the dome is visible, showing a complex internal structure and a circular opening at the top. The telescope is situated on a dark, circular platform. The background shows the reddish-brown landscape of Mars with hills and mountains under a hazy orange sky.

Thank you